

CHEMISTRY

Special Topic: Organic Chemistry Booming in China

Recent advances in visible-light-driven organic reactions

Qiang Liu¹ and Li-Zhu Wu^{2,*}

ABSTRACT

In recent years, visible-light-driven organic reactions have been experiencing a significant renaissance in response to topical interest in environmentally friendly green chemical synthesis. The transformations using inexpensive, readily available visible-light sources have come to the forefront in organic chemistry as a powerful strategy for the activation of small molecules. In this review, we focus on recent advances in the development of visible-light-driven organic reactions, including aerobic oxidation, hydrogen-evolution reactions, energy-transfer reactions and asymmetric reactions. These key research topics represent a promising strategy towards the development of practical, scalable industrial processes with great environmental benefits.

Keywords: visible light, catalysis, synthesis, photocatalyst, aerobic oxidation, hydrogen evolution, energy transfer, asymmetric photoreaction

INTRODUCTION

Since the pioneering chemist Giacomo Ciamician speculated the bright and broad future of photochemistry in 1900 [1], organic photochemistry has witnessed intense developments, which have gradually become an important synthesis tool. During the past decade, much progress has been made in the field of visible-light-driven organic reactions. Compared with relatively short-wavelength ultraviolet light, the advantages of visible light are obvious: (i) abundant in the solar spectrum, (ii) easily accessible for the equipment and (iii) fewer side reactions. Although most simple molecules are transparent to visible light, a wide range of transition metal complexes, as well as various organic dyes, have been productively exploited as efficient photocatalysts for the synthesis of complex organic structures. With an increasing understanding the roles of the photocatalysts, further exploitation of the photocatalysts accelerated the bloom of visible-light-driven organic reactions (Fig. 1).

Over the past several years, new powerful visible-light-driven synthetic methods have been favorites with organic chemists. There have been over 70 reviews focused on visible-light-driven organic reactions, which include the special issues of the *Accounts of Chemical Research* [2] and *Chemical Reviews* [3].

In this review, we briefly overview the recent research advances in the rapidly growing field, highlighting contributions in the new ‘golden age’ of photochemistry.

VISIBLE-LIGHT-DRIVEN AEROBIC OXIDATION

Molecular oxygen is a cheap, ecologically benign and most abundant oxidant. Recently, visible-light photocatalysis has offered a technically attractive and energy-saving platform for aerobic oxidation. With the aid of a photocatalyst excited by visible light, molecular oxygen could be activated to either singlet oxygen or superoxide radical anion by an energy-transfer or electron-transfer process. Both singlet oxygen and superoxide radical anion are reactive oxygen species (ROS) that may easily react with the substrates or the active species formed during the reaction (Fig. 2a). As a result, molecular oxygen may be involved in the products or transformed into hydrogen peroxide or water.

In 2010, Stephenson and co-workers reported the first photoredox-catalysed aza-Henry reaction by using Ir (III) bipyridine complex as the photocatalyst (Fig. 2c) [4]. Shortly afterwards, Rueping *et al.* combined photoredox catalysis and enamine catalysis to develop a dual catalytic system for

¹State Key Laboratory of Applied Organic Chemistry, Lanzhou University, Lanzhou 730000, China and ²Key Laboratory of Photochemical Conversion and Optoelectronic Materials, Technical Institute of Physics and Chemistry, Chinese Academy of Sciences, Beijing 100190, China

*Corresponding author. E-mail: lzww@mail.ipc.ac.cn

Received 20 January 2017; Revised 16 March 2017; Accepted 16 March 2017

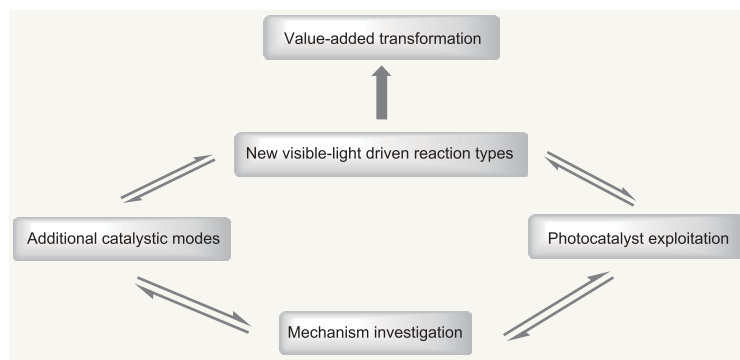


Figure 1. Outline of the strategies for value-added transformations driving by visible-light irradiation.

the Mannich reaction. Here, the combination of the photocatalyst Ru (II) complex and the Lewis base catalyst proline resulted in a high yield of the Mannich product (Fig. 2c) [5]. Later on, Xiao and co-workers exploited a visible-light-driven oxidation/[3 + 2] cycloaddition/oxidative aromatization sequence for the preparation of pyrrolo[2,1-a]isoquinolines (Fig. 2c) [6]. In these cases, tertiary amines, especially *N*-phenyl-tetrahydroisoquinolines, were employed as the substrates and the reactions were performed by visible-light irradiation of Ru (II)- or Ir (III)-based complexes under aerobic conditions. Although the iminium intermediate formed from the tertiary amines under the visible-light-driven aerobic conditions is believed to be responsible for the valuable transformations, the exact roles of molecular oxygen and ROS generated in the reactions were elusive at that time (Fig. 2b).

The subsequent reports from König [7], Tan [8] and our laboratory [9] demonstrated that the cheap organic dye eosin Y can be applied as an effective organo photocatalyst for the α -functionalization of tertiary amines in the presence of molecular oxygen (Fig. 2c). We disclosed the mechanism of the visible-light-driven aerobic oxidation by electron spin resonance (ESR) and flash photolysis. Although dyes, such as methylene blue or Rose Bengal (RB), were widely employed to photogenerate singlet oxygen by an energy-transfer process, ESR studies provide direct evidence for the formation of superoxide radical anions rather than singlet oxygen during visible-light irradiation of eosin Y in the presence of amines. This active species has been demonstrated to be responsible for the large rate of acceleration of the aerobic photocatalytic reactions. The results indicate that the traditional singlet-oxygen photosensitizers may be efficient electron-transfer photocatalysts if the free energy change of the photo-induced electron transfer between the excited photosensitizer and the substrate is thermodynamically feasible. Subsequently, platinum(II) terpyridyl com-

plex was founded to be a superior photocatalyst for aerobic cross-dehydrogenative-coupling reactions between *N*-phenyl-tetrahydroisoquinolines and nucleophiles. Here, the byproduct amine formed by the reaction of α -amino radical with ROS is completely eliminated with the aid of additive FeSO₄ (Fig. 2c) [10]. Recently, König and Gschwind disclosed the comprehensive picture of the reaction mechanism. The involved intermediates, reactive pathways of the amine radical cation and the influence of oxygen and the light source were fully investigated by NMR, ESR and synthetic methods [11].

The trapping of the electrophilic iminium ion or imine formed under the visible-light-driven aerobic conditions has been an efficient strategy to form C_{sp3}-C_{sp3} bonds. For example, Rueping and co-workers reported a visible-light-driven three-component reaction for the direct synthesis of α -amino amides and imides from tertiary amines (Fig. 2c) [12]. Iminiums, generated by aerobic oxidation using visible-light photoredox catalysis, were reacted with nucleophilic isocyanides to deliver nitrilium ions. Subsequent trapping of the nitrilium ions with water or carboxylic acid resulted in intermediates **I**, which rearranged to give the corresponding amides or imides, respectively. At the same time, our laboratory developed a dual catalytic protocol for the α -C-H functionalization of secondary glycine esters with β -keto esters (Fig. 2c) [13]. By combining the visible-light catalyst, Ru(bpy)₃Cl₂, and transition metal salts, Cu(OTf)₂, the photoreaction proceeded efficiently in the presence of molecular oxygen. In this reaction, we infer that superoxide radical anion generated from molecular oxygen is the active species participating in the reaction of secondary amines. The visible-light-driven aerobic oxidation was expanded to in-situ preparation of nitrones from hydroxylamines. In 2014, Rueping and co-workers disclosed oxidative [3 + 2] cycloaddition of *N*-substituted hydroxylamines with alkenes (Fig. 2c) [14]. Here, the aerobic oxidation of *N*-substituted hydroxylamines results in the formation of nitronium cations, which can easily isomerize to *N*-hydroxy iminium ion. Reaction of deprotonated *N*-hydroxy iminium ion with the alkenes yielded the [3 + 2] cycloaddition products isoxazolidines.

As shown in Fig. 2d, amines could be converted into the nitrogen-centered radical cations via visible-light-driven aerobic oxidation. The acidic radical cations were easily deprotonated to generate α -aminoalkyl radicals [15,16], which trend to add to alkenes bearing electron-withdrawing groups (EWGs). Yu and Bian reported aerobic oxidative cyclization of *N,N*-dialkylanilines with maleimides via α -aminoalkyl radicals [17]. Here, after addition of α -aminoalkyl radicals to maleimides, subsequent cyclization of the newly generated alkyl radical

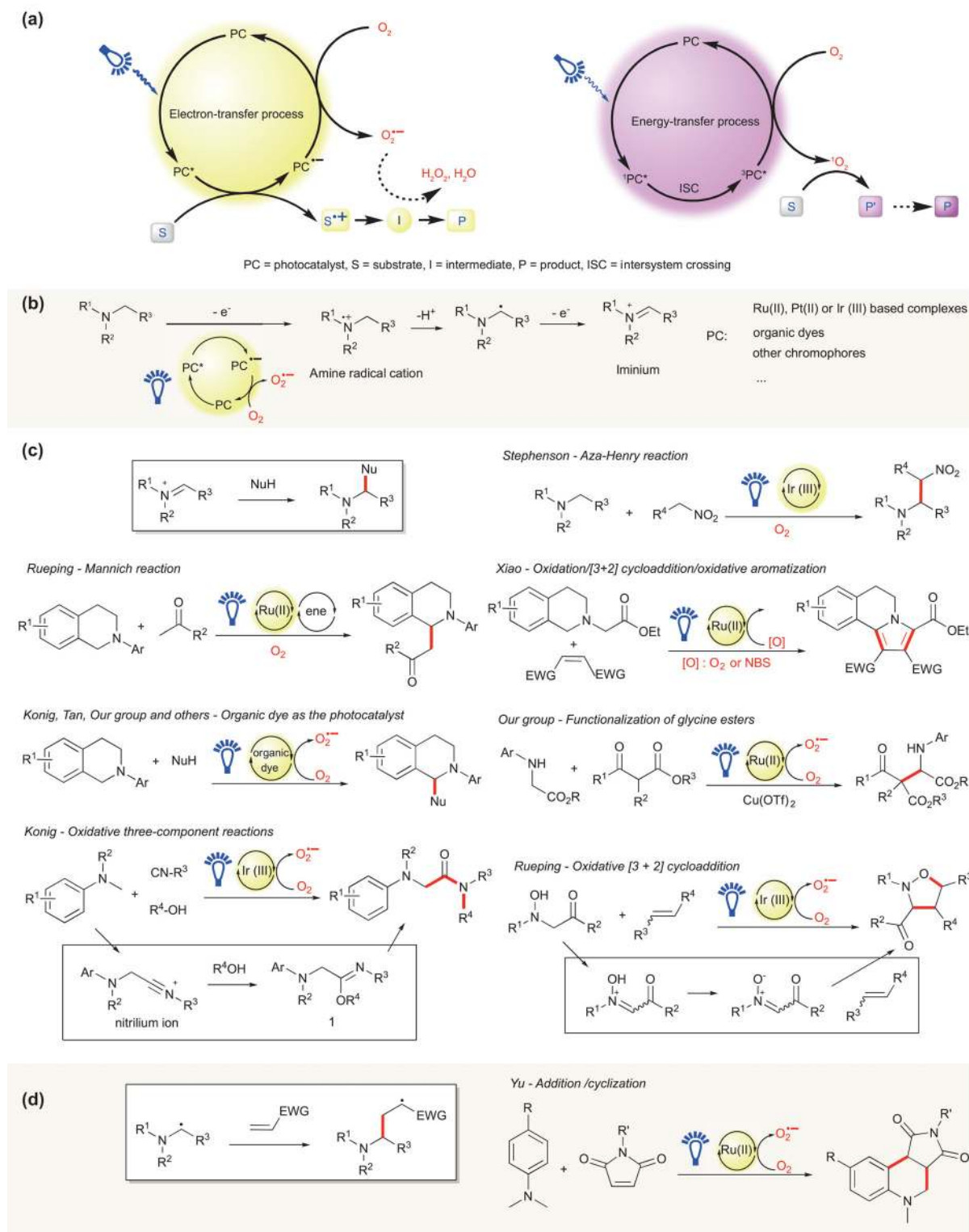


Figure 2. Visible-light-driven aerobic oxidation. (a) Outline of the pathways of visible-light-driven aerobic oxidation; (b) intermediates of amines in visible-light-driven aerobic oxidation; (c) the reactions of amines via iminium intermediates; (d) the reactions of amines via α -aminoalkyl radicals; (e) the reactions of amines via nitrogen-centered radical cations; (f) visible-light-driven aerobic C–C bond cleavage; (g) visible-light-driven aerobic C–H/C–N cleavage cascade; (h) the reaction of superoxide radical anion in visible-light-driven aerobic oxidation; (i) visible-light-driven aerobic oxidation with singlet oxygen; (j) trapping the ground state of molecular oxygen with carbon-centered radicals; (k) olefin-based cyclization using visible light and molecular oxygen.

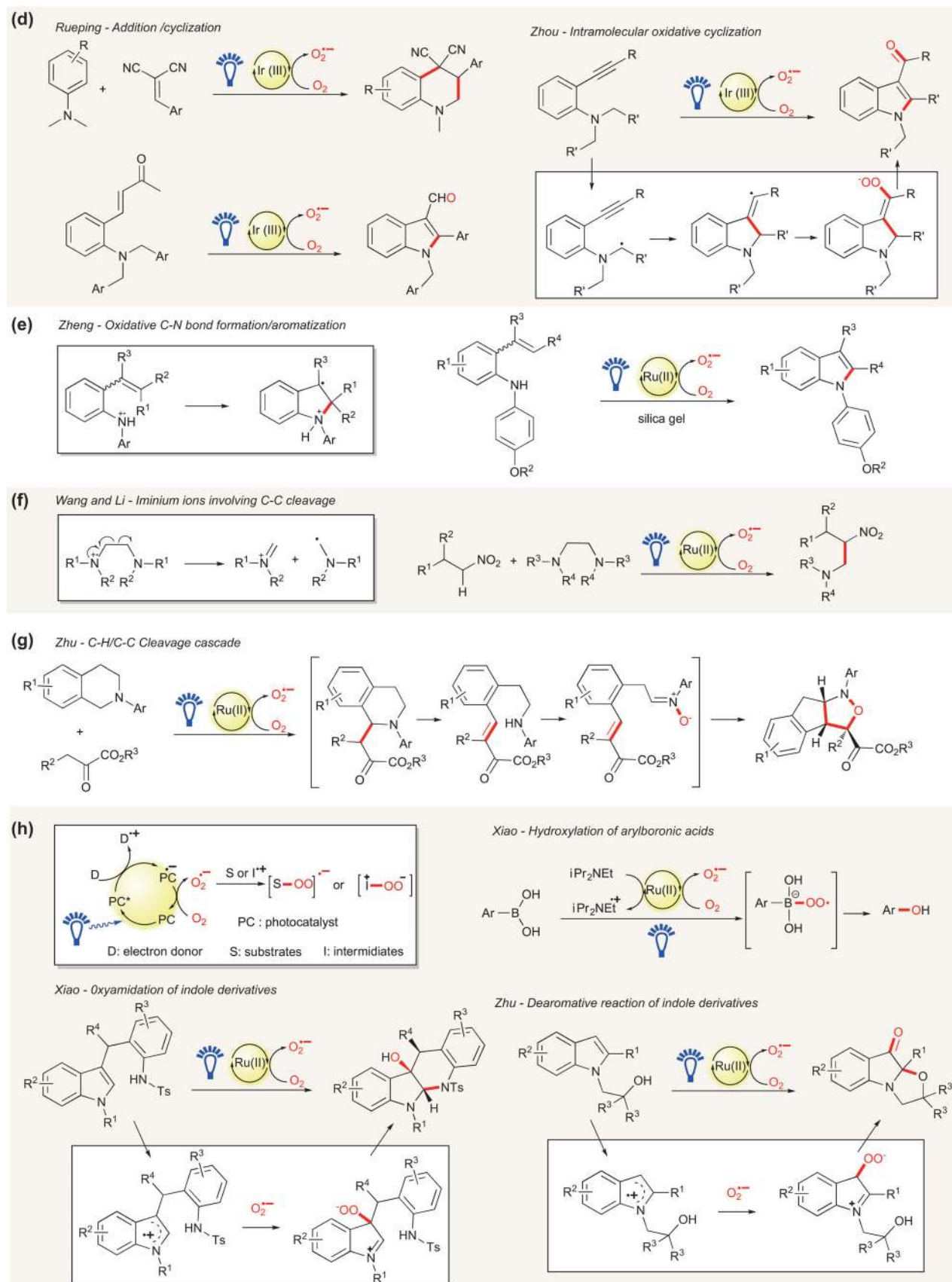


Figure 2. Continued.

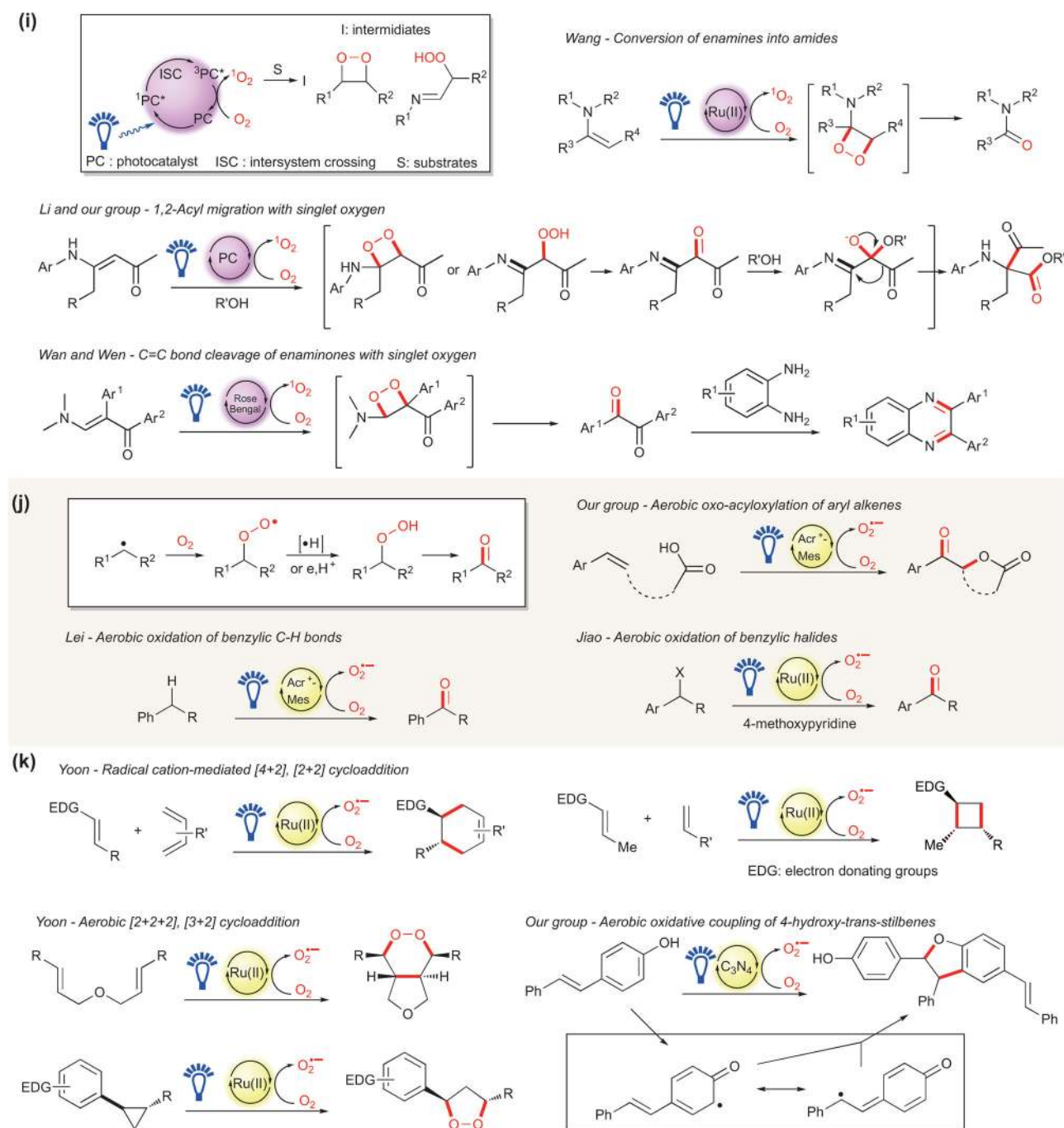


Figure 2. Continued.

intermediates with neighboring aniline rings gives the corresponding 1,2,3,4-tetrahydroquinoline derivatives (Fig. 2d). Similar reactions under visible-light-driven aerobic oxidation were reported by Rueping and co-workers [18]. The visible-light-driven aerobic synthesis of indole-3-carbaldehydes through a sequential C–C bond formation/aromatization/carbon–carbon bond

cleavage process involving α -amino alkyl radicals was also disclosed. In these protocols, molecular oxygen and the generated superoxide radical anion were crucial for the rearomatization. Zhou *et al.* also developed intramolecular cyclization based on the addition of α -aminoalkyl radicals to alkynes (Fig. 2d) [19]. In the transformation, the vinyl radicals, formed by the addition of α -aminoalkyl radicals

to the alkyne moiety, further reacted with molecular oxygen or superoxide radical anion. Subsequent carbon–carbon bond cleavage of the peroxides resulted in corresponding indol-3-yl ketones.

The utility of nitrogen-centered radical cations that are generated through visible-light-driven aerobic oxidation of the corresponding anilines has also been recognized in C–N bond formation (Fig. 2e) [20]. In 2012, Zheng described that a nitrogen-centered radical cation, which is generated from styryl aniline, can undergo electrophilic addition to the tethered alkene, thus triggering a cascade reaction involving aromatization. This chemistry marked a new way to use photogenerated amine radical cations to the preparation of fused indoles and indolines using mild, aerobic conditions. Later on, the strategy using nitrogen-centered radical cation activation has been extended to generate substituted pyrrolidines and piperidines through olefin hydroamination [21].

Besides the well-known deprotonation process triggered by visible-light-driven aerobic oxidation, C–N bond cleavage or C–C bond cleavage adjacent to the nitrogen-centered radical cation is also feasible if proper amines and reaction conditions are employed. Visible-light-promoted C–C bond cleavage was achieved by Li and Wang through employment of simple vicinal diamines as precursors of nitrogen-centered radical cations [22]. The presence of a β -nitrogen atom in close proximity to the *N*-centered radical cations led to the cleavage of the central C–C bond as well as concomitant formation of both iminium ions and α -aminoalkyl radicals. Subsequent trapping of the iminium ions with nucleophilic nitro substrates resulted in aza-Henry products (Fig. 2f). In 2013, Zhu's group reported a visible-light-driven aerobic C–H/C–N cleavage cascade to isoxazolidine skeletons. Here, the adducts of iminium ions with α -ketoesters undergo C–N cleavage via a retro-aza-Michael reaction. Under aerobic oxidative conditions, the formed amine intermediates can be oxidized to nitrile oxides, which produce the desired bicyclic isoxazolidines by an intramolecular [3 + 2] cycloaddition (Fig. 2g) [23].

The superoxide radical anion generated from the photoredox cycle is active to substrates or intermediates with strong Lewis acidity and low electronegativity (Fig. 2h). Xiao and co-workers described that the superoxide radical anion, produced by employing a Ru(II) complex or eosin Y as the photocatalyst and diisopropylethylamine (*i*Pr₂NEt) as the sacrificial electron donor, could react with arylboronic acids. Further rearrangements of the superoxide radical anion adducts provided aryl alcohols (Fig. 2h) [24]. Later on, Scaiano reported the use of methylene blue as the photocatalyst for the oxidative hy-

droxylation of arylboronic acids (Fig. 2h) [25]. In other work, Xiao reported visible-light-driven aerobic oxyamidation of indole derivatives involving the reaction of electrophilic indolyl radical cations with the superoxide radical anion. Subsequent intramolecular cyclization and O–O bond cleavage afforded tetrahydro-5*H*-indolo [2,3-*b*]quinolinols (Fig. 2h) [26]. In a concomitant report, Zhu and co-workers demonstrated that this strategy could be used to achieve the dearomatization of indoles, providing a straightforward synthesis of heterocycle fused or spirocyclic indolones (Fig. 2h) [27]. Similarly, the group of Xia disclosed visible-light-mediated aerobic oxidative C–C bond cleavage of aldehydes. Here, the enamines formed in situ from aldehydes and secondary amines were oxidized to radical cations, which were reacted with superoxide radical anion to afford the desired products [28].

The energy gap between singlet oxygen and its ground-state triplet is around 22.5 kcal/mol [29], which is lower than the lowest triplet energy of many excited photocatalysts. Therefore, in most cases, for visible-light-driven aerobic oxidation, the generation of singlet oxygen is sufficient. Generally, the multiple parallel pathways of singlet oxygen such as the 'ene' reaction, cycloaddition and heteroatom oxidation often give rise to complicated oxygenated products [30]. So far singlet oxygen has been employed to realize only a few organic transformations in visible-light-driven aerobic oxidation (Fig. 2i). In 2014, Wang and co-workers disclosed visible-light-driven conversion of enamines into amides. The reaction is believed to involve a singlet-oxygen-mediated [2 + 2] cycloaddition. Subsequent carbon–carbon and peroxy bond cleavage of 1,2-dioxetanes afforded amides (Fig. 2i) [31]. Shortly after, Li [32] and our laboratory [33] independently reported that visible-light-mediated aerobic oxidation of secondary enamines by singlet oxygen could afford quaternary amino acid derivatives through the process of 1,2-acyl migration (Fig. 2i). Here, an ene-type reaction or [2 + 2] cycloaddition between enamines and singlet oxygen occurs. The desired products are formed by a nucleophilic addition of alcohol to 1,2-diketone intermediates followed by 1,2-acyl migration. Tetraphenylporphyrin, RB, and Ru(II)- or Pt(II)-based complexes are efficient photocatalysts for the transformation. The reaction provides a mild and simple protocol to amino acid derivatives with a quaternary carbon. It is worth noting that, following the above publications, Fu and Shang demonstrated that stable 1,2-diaryldiketones could be generated from enamines through carbon–carbon and peroxy bond cleavage of 1,2-dioxetanes formed by singlet-oxygen-mediated [2 + 2] cycloaddition. Further

reaction of the in-situ-generated 1,2-diketones with diamines afforded quinoxalines [34].

The ground-state molecular oxygen is triplet. It couples readily with carbon-centered radicals generated from the visible-light-driven aerobic oxidations due to its diradical character. The resulting peroxide radicals further transform into corresponding peroxides through hydrogen-atom abstraction or electron transfer following proton transfer. Finally, the elimination of water of the peroxides furnishes corresponding ketones (Fig. 2j). In 2016, our laboratory reported a visible-light-driven oxoacyloxylation of aryl alkenes with carboxylic acids and molecular oxygen. In this work, 9-mesityl-10-methylacridinium perchlorate (Mes-Acr⁺) was employed as the photocatalyst to inhibit the generation of singlet oxygen. The alkene radical cations, produced by the single-electron transfer from alkenes to the excited singlet state of Mes-Acr⁺, were trapped by the carboxyl anion and molecular oxygen, respectively [35]. Prior to this report, similar strategies had been used to achieve the visible-light-driven aerobic oxidation of benzyl halides [36] and benzylic sp³ C–H compounds [37].

In 2011, Yoon and co-workers investigated visible-light-driven [4 + 2] cycloaddition of electron-rich olefins with electron-rich dienes under ambient air (Fig. 2k) [38]. Here, molecular oxygen was employed as the electron acceptor to complete the photoredox cycle and regenerate the photocatalyst. Compared with the reaction under an anaerobic condition, the concentration of radical cation in the aerobic condition was improved, thereby facilitating catalyst turnover and enhancing the yield of the cycloaddition. In a similar vein, they realized radical cation-mediated crossed [2 + 2] cycloaddition by using visible light and molecular oxygen (Fig. 2k) [39]. Following on from these reports, [2 + 2 + 2] aerobic cycloaddition of bis(styrene) substrates was achieved by increasing the concentration of molecular oxygen and lowering the reaction temperature (Fig. 2k) [40]. This methodology provides an attractive approach to the production of endoperoxides. Similarly, a range of five-membered endoperoxides could be prepared in excellent yield by [3 + 2] cycloaddition of aryl cyclopropanes with molecular oxygen [41]. In 2014, we showed that visible-light-driven aerobic oxidative coupling of 4-hydroxy-*trans*-stilbenes could be accomplished using mesoporous graphitic carbon nitride (mpg-C₃N₄) as the photocatalyst through a radical–radical coupling pathway (Fig. 2k). Generation of the active quinone methide radical could occur via photo-induced electron transfer from a phenolate anion, which was produced by ionization of 4-hydroxy-*trans*-stilbene in the presence of

2,6-lutidine. The coupling of the quinone methide radical and its resonance structure, a benzyl radical, followed by tautomeric rearrangement and intramolecular nucleophilic attack to the methylene of the intermediate semiquinone gave the dimer with a dihydrobenzofuran skeleton [42]. In this work, the acceleration of the reaction by 2,6-lutidine was attributed to the increased phenolate anion generated by the ionization of 4-hydroxy-*trans*-stilbenes. The results indicate that, for the compounds containing labile protons, the introduction of proper bases significantly contributes to the electron transfer from substrates to the excited photocatalysts, thereby suppressing the side-reaction of singlet oxygen. This strategy has been extended to aerobic aromatization of 1,4-dihydropyrimidines 1,4-dihydropyridines and synthesis of 2-arylbenzoxazoles [43,44].

VISIBLE-LIGHT-DRIVEN HYDROGEN-EVOLUTION REACTION

As discussed in the previous section, inter- or intramolecular dehydrogenation could proceed via electron-transfer-mediated oxidations. Organic compounds such as amines could easily be oxidized into the corresponding radical cations via visible-light-driven oxidation. In most cases, the radical cations are highly acidic and could be deprotonated to generate radical intermediates. Subsequent reactions triggered by the intermediates provide meaningful dehydrogenative products. The reaction involves loss of two electrons and two protons, which could produce hydrogen gas theoretically. In fact, hydrogen gas is not usually the byproduct due to the thermodynamics difficulty of building a carbon–carbon bond with the loss of hydrogen. Therefore, an appropriate sacrificial oxidant is usually required to promote the transformation. However, the use of stoichiometric sacrificial oxidants leads to low atom economy, possible generation of toxic wastes and the side reactions caused by the oxidant intercalation. In recent years, there has been an intense effort to develop hydrogen-evolution catalysts (HEC) for light-induced splitting of water [45]. The employment of a hydrogen-evolution catalyst as an acceptor of electrons and protons in dehydrogenation not only provides an oxidant-free strategy, but also yields hydrogen gas—a useful energy resource—as the sole byproduct.

Visible-light-driven hydrogen evolution from Hantzsch 1,4-dihydropyridine derivatives in homogeneous systems was first reported by our laboratory [46]. In this work, platinum (II) terpyridyl complexes were used as the sole catalyst.

The reaction was initiated by singlet electron transfer from substrates to excited platinum (II) terpyridyl complexes followed by a proton-coupling hydrogen-evolution process. In a similar vein, we realized visible-light-driven synthesis of 3,4-disubstituted pyrroles [47], 3,4-diarylthiophenes [48] and 1,3,5-triaryl pyrazoles [49] with hydrogen gas as the sole byproduct.

In recent decades, dehydrogenative cross-coupling is becoming a highly desirable synthetic approach to construct C–C bonds directly, as it does not require prefunctionalization and defunctionalization of subcomponents. Typically, an appropriate sacrificial oxidant is usually required to promote the transformation. To obviate the need for an external oxidant, we develop a visible-light-driven catalytic system named cross-coupling hydrogen evolution (CCHE), in which the two electrons and two protons generated in the dehydrogenative cross-coupling process are transformed to hydrogen gas by an appropriate hydrogen-evolution catalyst (Fig. 3a). In 2013, we realized the first example of visible-light-driven CCHE between a variety of *N*-phenyl-tetrahydroisoquinoline and indole substrates [50]. Here, eosin Y and a grapheme-supported RuO₂ nanocomposite (G-RuO₂) were employed as the photocatalyst and the HEC, and this dual-catalyst system can afford excellent yields of cross-coupling products and an equivalent amount of H₂. Mechanism research demonstrated that eosin Y participated in the photo-induced electron-transfer process and G-RuO₂ captured the electron and proton released from the substrates. The trapping of the electrophilic iminium ions by indoles furnished the products (Fig. 3b). A subsequent report showed that a cobaloxime Co(dmgh)₂Cl₂ could be employed as the hydrogen-evolution catalyst, providing an improvement in the yield of many substrates and a noble-metal-free CCHE system [51]. Mechanism studies indicated that the molecular hydrogen-evolution catalyst Co(dmgh)₂pyCl (Co(III)) captured two electron populated highly active Co(I) species. The Co(I) species then were reacted with protons to produce substantially stabilized Co(III)-H species, which could generate hydrogen gas and low-valence cobalt species (Fig. 3b).

Later on [52], we expand the scope of substrates from tertiary amines tetrahydroisoquinolines to secondary amines glycine esters by combining Ru(bpy)₃(PF₆)₂ as the photosensitizer and Co(dmgh)₂PyCl as the hydrogen-evolution catalyst. The visible-light-driven CCHE reaction of glycine esters with β -keto esters or indole derivatives afforded cross-coupling products in good to excellent yields (Fig. 3b). In a further demonstration

of the utility of CCHE, the cross-coupling between isochromans and β -keto esters was performed [53]. By employing a more strongly oxidizing photocatalyst 9-mesityl-10-methylacridinium perchlorate (Mes-Acr⁺), isochromans could be converted into oxocarbenium ions. Further nucleophilic addition of the oxocarbenium species by β -keto esters in the presence of Cu(OTf)₂ produced the desired coupling products (Fig. 3b).

The construction of carbon(sp²)-sulfur bond-forming benzothiazoles via intramolecular CCHE was developed by Lei and our group in 2014 [54]. In this work, the aromatic carbon–hydrogen bond thiolation was based on the electron and proton transfer in the [Ru(bpy)₃]²⁺/Co(dmgh)₂(p-NMe₂Py)Cl system, and the employment of an appropriate base was crucial for the efficiency of the reaction. The unexpected oxidation byproduct amides, which are often generated in oxidative cyclization of thiobenzanilides, can be completely avoided (Fig. 3b). More recently [55], we disclosed a visible-light-driven CCHE strategy for indole synthesis using *N*-aryl enamines as the starting materials. The reaction was triggered by the electron transfer from the excited photocatalyst Ir(ppy)₃ to the cobaloxime complex Co(dmgh)₂(4-CO₂Mepy)Cl, which can generate strongly oxidizing Ir(IV). Therefore, the oxidation of *N*-aryl enamines with Ir(IV) could take place in the absence of any base. Subsequent intramolecular radical addition yielded the indoles smoothly under CCHE conditions (Fig. 3b).

In a further demonstration of the utility of CCHE, our groups showed that the inert C–H bond of benzene could be directly functionalized by ammonia and water under light-driven CCHE conditions [56]. The crucial step for the initiation of the CCHE is the activation of benzene by electron-transfer oxidation. To this end, 1-methylquinolinium ion (QuH⁺) and 3-cyano-1-methylquinolinium ion (QuCN⁺) were selected as the photocatalysts. The benzene radical cations were produced via a single-electron transfer process and attacked by nucleophile OH[−] or [−]NHR to give a dienyl radical. Subsequently, the dienyl radical lost an electron and underwent deprotonation, thereby affording aniline and phenol. At the same time, two electrons and two protons produced during the amination or hydroxylation were transformed to hydrogen gas in the presence of HEC Co(dmghBF₂)₂(CH₃CN)₂ (Fig. 3b). Along similar lines, Lei and co-workers utilized Mes-Acr⁺ (9-mesityl-10-methylacridinium) and Co(dmghBF₂)₂(CH₃CN)₂ as a photocatalytic system and realized the addition of high-activity styrenes with water affording the corresponding carbonyl compounds (Fig. 3b) [57]. Herein, the alkene radical cation

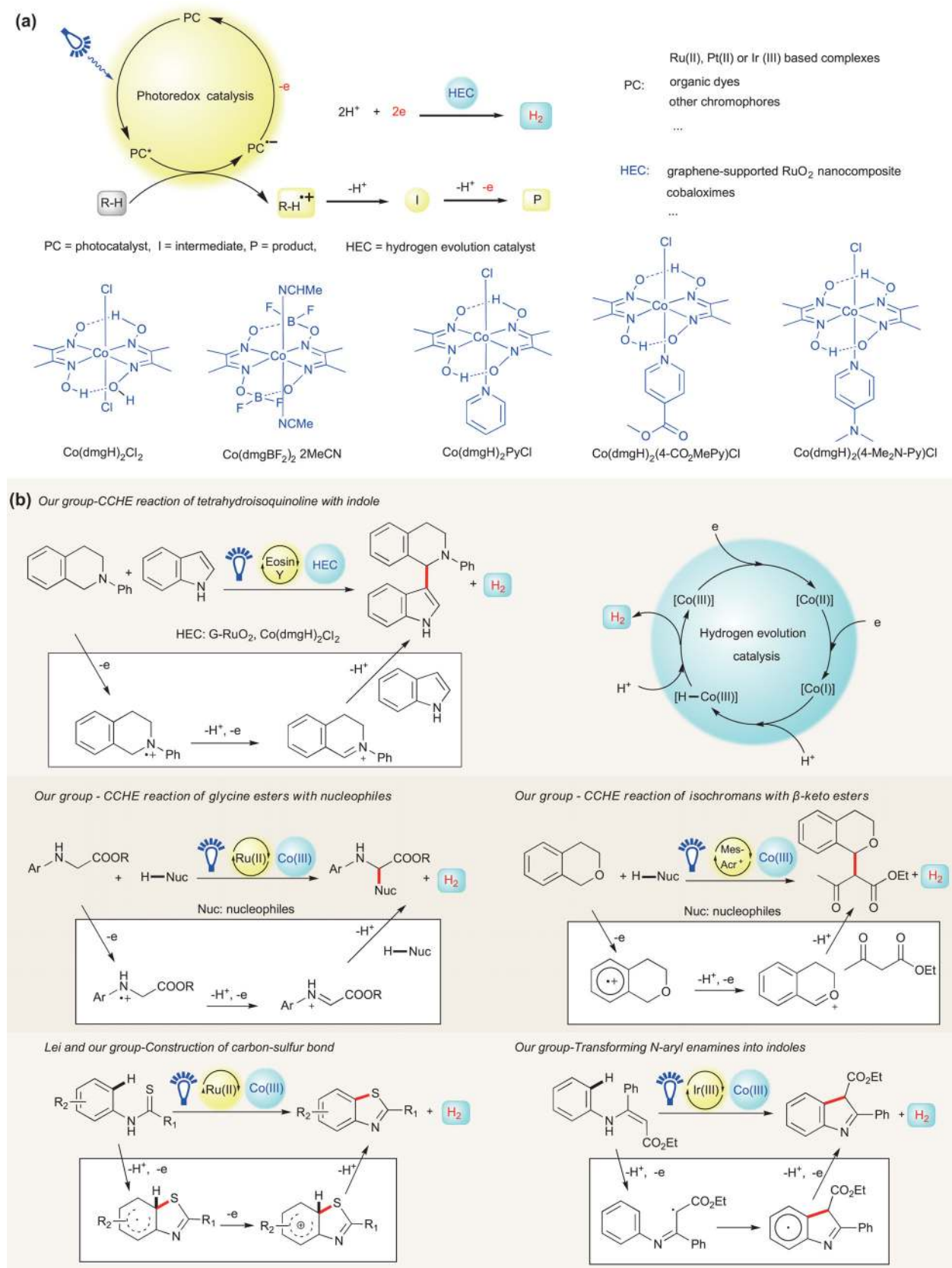


Figure 3. Visible-light-driven coupling hydrogen evolution reactions. (a) Outline of the pathway; (b) inter- or intramolecular coupling hydrogen-evolution reactions in dual catalytic system; (c) hydrogen-evolution reactions in monocatalytic system.

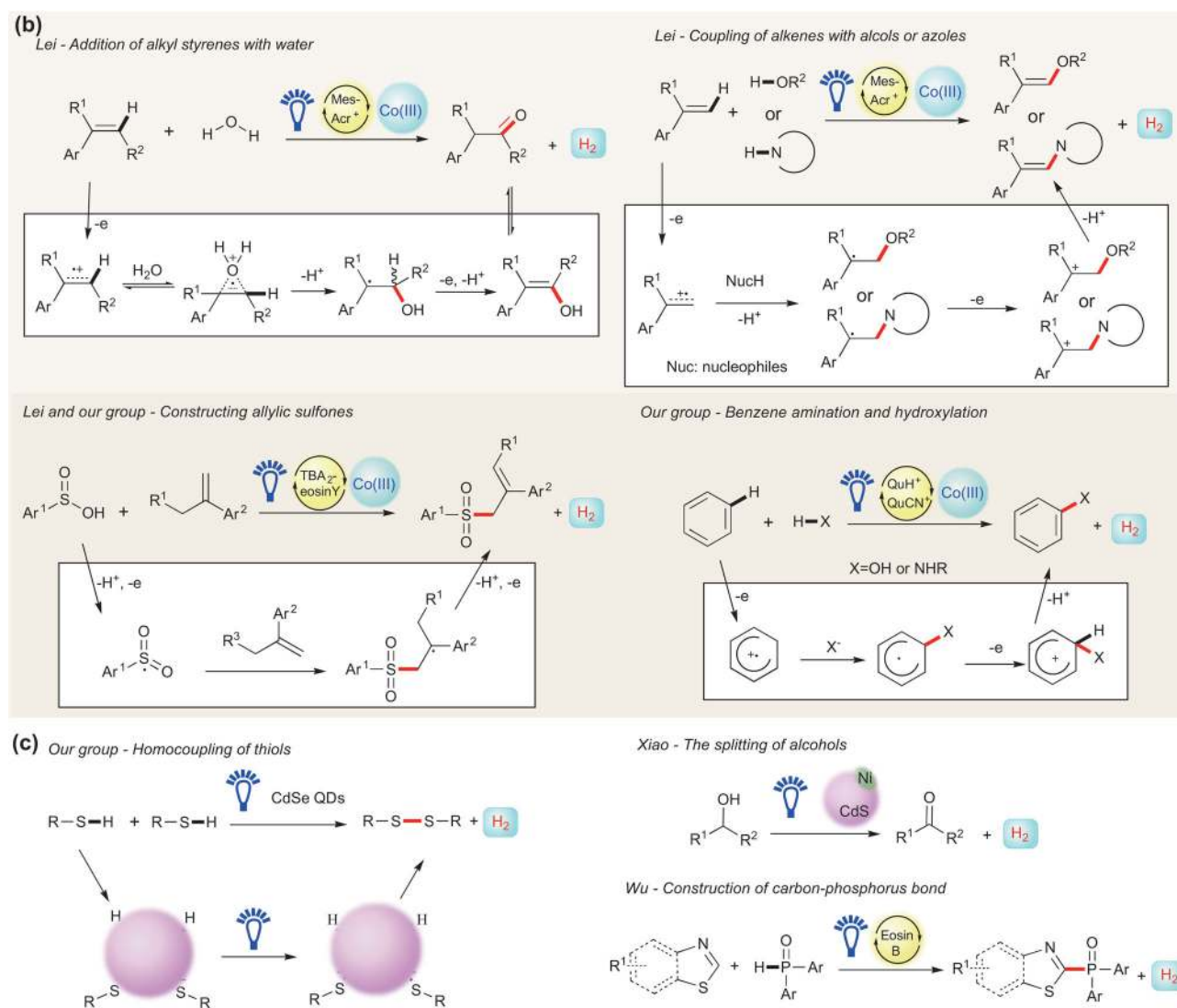


Figure 3. Continued.

intermediate generated by a single electron from the alkene to the excited Mes-Acr⁺ controlled the regioselectivity. Subsequently, they coupled alcohols and azoles with styrenes and constructed enol ester derivatives and *N*-vinylazoles successfully in the same system (Fig. 3b) [58]. Here, alkenes were employed as redox substrates and alcohols or azoles were employed as nucleophiles to trap the crucial alkene radical cations intermediate. Later on, Lei and our group reported the synthesis of allylic sulfones via the CCHE of aryl sulfonic acid and limited α -methyl-styrene derivatives in the TBA₂-eosin Y/Co(dmgH)₂pyCl system (Fig. 3b) [59]. Deprotonation of aryl sulfonic acid in the presence of the base pyridine generated corresponding pyridinium sulfinate, which could be transformed to active sulfonyl radical by electron transfer from pyridinium

sulfinate to the excited eosin Y. The resultant sulfonyl radical is electrophilic and is readily trapped by α -methyl-styrene derivatives to ultimately deliver allylic sulfones.

In 2014, our group first utilized CdSe QDs (quantum dots) as the catalyst to transfer thiols into disulfides and hydrogen gas under visible-light irradiation (Fig. 3c) [60]. In this work, deprotonated thiols bound to the surface through cadmium-sulfur bonds to form QD/thiolate conjugates. The thiol radicals produced via the oxidation of thiol anions by photo-induced QDs holes. After the homocoupling of thiol radicals, the generated disulfides were dissociated from the surface of the QD, thereby avoiding the overoxidation of the thiols. Meanwhile, the protons were reduced to hydrogen atoms stabilizing on the QD surfaces by the conduction band,

furnishing hydrogen gas as the sole byproduct. In particular, the addition of nickel(II) salts greatly improved the conversion of thiols and the hydrogen emission by providing more sites on the QDs surface for proton reduction. In a subsequent report, Ni-modified CdS QDs were demonstrated as a competent catalyst for splitting alcohols into hydrogen and corresponding aldehydes or ketones in a stoichiometric manner under visible-light irradiation (Fig. 3) [61]. Similarly, the absorption of alcohol on the Ni particle surface and the electron transfer between Ni nanocrystals and CdS played pivotal roles in the visible-light-driven dehydrogenation system. The results raise the exciting prospect of heterogeneous photocatalysts in developing highly efficient monocatalytic hydrogen-evolution protocols. Prior to this work, a monocatalytic system using organic dye eosin B as the sole catalyst for the visible-light-driven CCHE reaction of thiazole derivatives with diarylphosphine oxides has been explored (Fig. 3c) [62].

VISIBLE-LIGHT-DRIVEN SYNTHESIS BY ENERGY-TRANSFER PROCESSES

In most of the recently reported visible-light-driven reactions, the substrates are activated by single-electron transfer between the excited photocatalysts and the substrates. Molecules that cannot undergo single-electron transfer with photocatalysts would be unreactive under such conditions. One effective strategy to overcome this obstacle is to use the excited triplet photocatalysts to convert the substrates into their triplet states via energy transfer. In these cases, successful activation depends on the relative triplet-state energies of the photocatalysts and substrates, and not on redox potentials. At first, irradiation of visible light excites a suitable triplet photocatalyst from its ground singlet state (S_0) to its lowest singlet excited state (S_1). And thereafter, the long-lived lowest-energy triplet state (T_1) is generated by intersystem crossing (ISC). Finally, the decay of triplet photocatalyst from its triplet state to its ground singlet state promotes substrates from its ground singlet state (S_0) to its lowest-energy triplet state (T_1) via a triplet–triplet energy-transfer process (Fig. 4a). The dominating mechanism for photocatalytic activation of organic substrates via energy transfer is the Dexter electron-exchange mechanism [63]. While the photo-induced electron exchange between photocatalysts and organic substrates occurs, the energy transfer is simultaneously accompanied. Because of the existence of relatively long-lived triplet metal-to-ligand charge transfer states

under visible-light irradiation, the well-known octahedral complexes such as Ru (II)- and Ir (III)-based complexes are possible candidates for such photocatalysts. To date, some seminal work involved in the energy-transfer mechanism has been reported.

The triplet-state alkenes are important intermediates in many long-known photoreactions such as photosensitized *cis*–*trans* isomerization, photorearrangement and photocycloadditions. In general, such processes originate from a thermally relaxed triplet produced by the energy transfer between photocatalysts and alkenes. As early as 1973, Markham reported that triplet-state $\text{Ru}(\text{bpy})_3^{2+}$ could be quenched by olefins such as anthracene, stilbene and styrylpyridines. The efficient triplet–triplet energy-transfer process led to *cis*–*trans* isomerization of the olefins [64]. In 1986, Yamazaki utilized the same photocatalyst to transform the substituted norbornadienes to quadricyclenes by the triplet energy transfer (Fig. 4b) [65]. Here, the norbornadiene accepts triplet–triplet energy from the excited $\text{Ru}(\text{bpy})_3^{2+}$ to populate its triplet state, which then undergoes bond rearrangement to give the corresponding quadricyclene. Visible-light activation of alkenes by triplet–triplet energy transfer can be also accomplished by using $\text{Ir}(\text{ppy})_3$ or other Ru (II) complexes as the photocatalyst. For instance, the *trans*–*cis* isomerization of trifluoromethylated alkenes was found during the visible-light-driven trifluoromethylation of styrenes using $\text{Ir}(\text{ppy})_3$ as the catalyst (Fig. 4b) [66]. Similarly, the isomerization of 4-cyanostilbene could be achieved by a bimetallic complex $[\text{CpRu}(\text{CH}_3\text{CN})(\text{CO})(\text{Pru})]^{3+}$ (Cp = cyclopentadiene) (Fig. 4b) [67]. The Castellano laboratory demonstrated that the triplet anthracene could be formed by excitation of $\text{Ru}(\text{dmb})_3^{2+}$ (dmb = 4,4'-dimethyl-2,2'-bipyridine) [68]. In 2015, Inagaki and co-workers designed a binuclear Ru–Pd complex in which a 2,2'-bipyrimidine ligand coordinates both a photoactive ruthenium center and a catalytically active palladium center. Under visible-light irradiation, energy transfer from the chromophore ruthenium center to the palladium center promoted migratory insertion of a second equivalent of α -methylstyrene, leading to dimerization of α -methylstyrene in excellent yield [69].

In 2012, Xiao disclosed a highly diastereoselective and regioselective [2 + 2] cycloadditions of 3-ylideneoxindoles through the energy-transfer pathway (Fig. 4c). In this work, excitation of $\text{Ru}(\text{bpy})_3^{2+}$ populated triplet 3-ylideneoxindoles, which react with the singlet ground-state ones to form the dimeric products via a 1,4-biradical intermediate [70]. In the same year, Yoon reported triplet–triplet

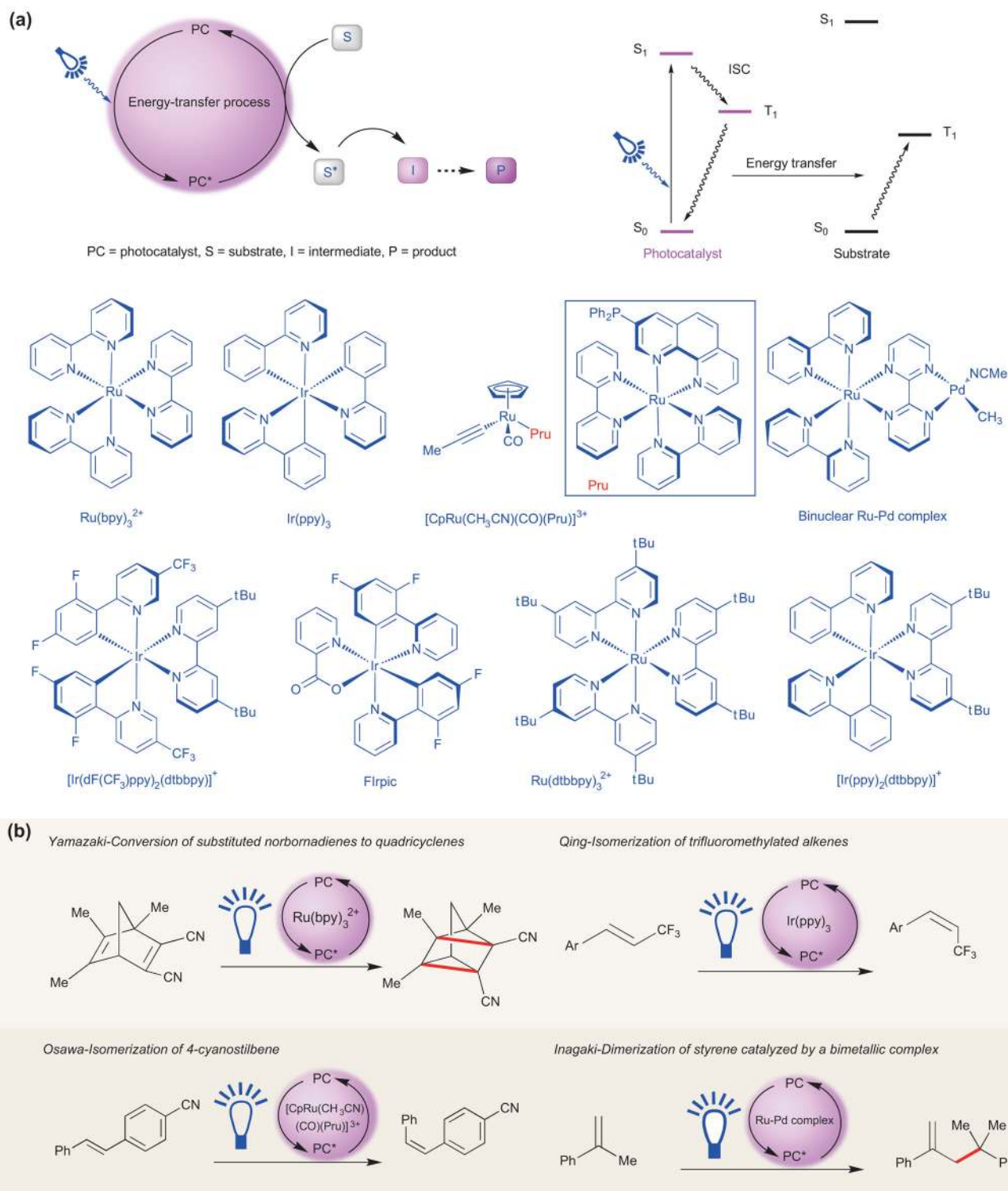
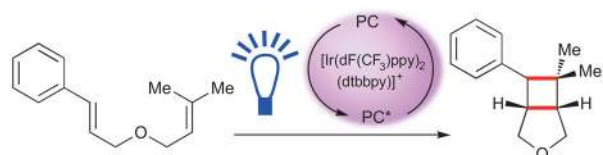


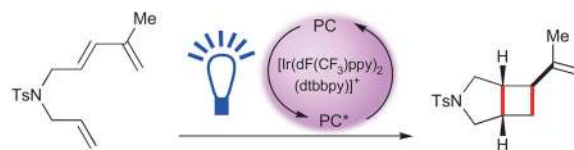
Figure 4. Visible-light-driven synthesis by energy-transfer processes. (a) Mechanism of energy-transfer processes; (b) visible-light-driven rearrangement, isomerization and dimerization; (c) photocatalytic [2 + 2] cycloadditions; (d) visible-light-driven azidations via nitrenes intermediate process; (e) visible-light-driven Ullmann-type C–N cross-coupling and silyl enol ether protonation.

(c) Xiao-[2+2] Cycloaddition of 3-ylideneoxindoles

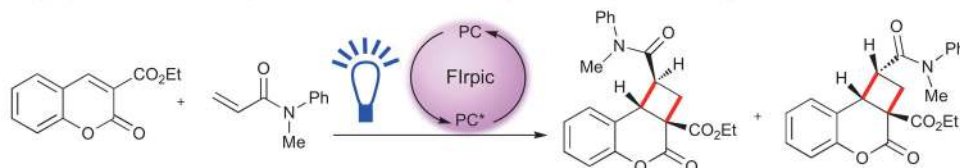
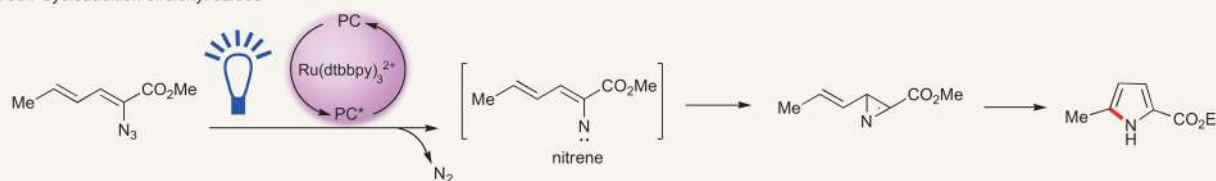
Yoon-[2+2] Cycloaddition of styrenes



Yoon-[2+2] Cycloaddition of 1,3-dienes



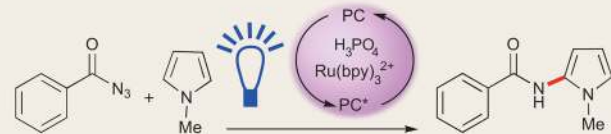
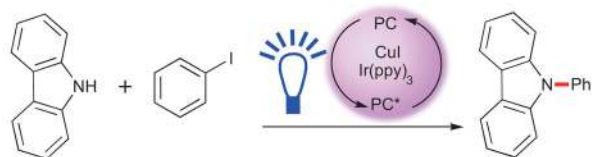
Our group-Intermolecular [2+2] cycloadditions of coumarin-3-carboxylates and acrylamides analogs

**(d)** Yoon-Cycloaddition of diene azides

Yoon-Chemoselective intermolecular aziridination



König - Arene C-H amination via Ru and Brønsted acid cocatalysis

**(e)** Fu and Peters-Ullmann-type C-N cross-coupling by Ir/Cu dual catalysis

Hanson-Silyl enol ether protonation by Ir and Naphthol cocatalysis

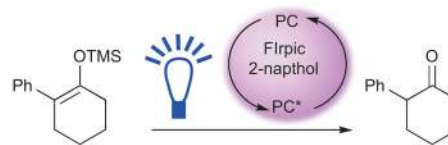


Figure 4. Continued.

energy transfer to achieve the [2 + 2] cycloadditions of styrenes using the iridium photocatalyst $\text{Ir}[\text{dF}(\text{CF}_3)\text{ppy}]_2(\text{dtbbpy})^+$ (Fig. 4c) [71]. As styrenes possess an excited-state triplet energy of 60 kcal/mol, $\text{Ir}[\text{dF}(\text{CF}_3)\text{ppy}]_2(\text{dtbbpy})^+$ acts as a suitable catalyst that has a triplet energy of approximately 61 kcal/mol and could be capable of

activating styrenes via energy transfer. Here, highly electron-deficient alkenes such as a 4-nitrostyrene and a 2-pyridylstyrene that are unfavorable for electron-transfer-mediated [2 + 2] cycloadditions efficiently produced the desired products. In a subsequent report, Yoon demonstrated that this strategy would also be suitable for [2 + 2] dienes

photocycloadditions (Fig. 4c) [72]. Dienes are also difficult to undergo single-electron oxidation, as well as styrenes. Because the lowest triplet-state energy of 1,3-dienes is around 55–60 kcal/mol, the same photocatalyst $\text{Ir}[\text{dF}(\text{CF}_3)\text{ppy}]_2(\text{dtbbpy})^+$ could be used to activate simple conjugated dienes, thereby accomplishing synthetically valuable vinylcyclobutane products. Along similar lines, our laboratory utilized the iridium complex FIrpic as the photocatalyst to realize visible-light-driven intermolecular [2 + 2] enone cycloadditions (Fig. 4c). A wide range of cyclobutabenzocopyranones were synthesized from coumarin-3-carboxylates and acrylamides in moderate to excellent yields [73].

In a seminal publication from Yoon, the generation of nitrenes was reported based on a triplet azide decomposition, wherein the ground state of di-enyl azides could be transformed to its excited triplet state by energy transfer from the $\text{Ru}(\text{bpy})_3^{2+}$ triplet state (Fig. 4d). The nitrene intermediate can subsequently cyclize onto another intermediate azirine, which undergoes slow but high-yielding rearrangement to the desired pyrroles [74]. In a subsequent report, Yoon accomplished visible-light-driven intermolecular alkene aziridination by the reaction of alkenes with nitrenes derived from azidoformates (Fig. 4d) [75]. The triplet nitrenes are formed through energy transfer from the excited state of $[\text{Ir}(\text{ppy})_2(\text{dtbbpy})]^+$ to 2,2,2-trichloroethyl azidoformates. With this methodology, a wide range of aliphatic and aromatic alkenes can be readily aziridinated without competitive allylic insertion reactions. Moreover, König and co-workers reported the direct C–H amidation of electron-rich heteroarenes with benzoyl azides in the presence of $\text{Ru}(\text{bpy})_3\text{Cl}_2$ and Brønsted acid (Fig. 4d) [76]. The excited $\text{Ru}(\text{bpy})_3\text{Cl}_2$ activated benzoyl azides to generate free nitrenes via the energy-transfer process. Protonation of the benzoyl nitrenes under the strongly acidic conditions gives electrophilic nitrenium ions, which react with the electron-rich heteroarenes such as pyrroles, indoles, furans, benzofurans and thiophenes. Further rearomatization afforded the corresponding amide coupling products in moderate to good yields.

In 2015, Kobayashi and co-workers reported the Ullmann-type C–N cross-coupling reaction between carbazole derivatives and aryl iodides using the dual-catalyst system of $\text{Ir}(\text{ppy})_3$ and $\text{Cu}(\text{I})$ under mild visible-light conditions (Fig. 4e) [77]. In this process, two carbazole anions coordinated with $\text{Cu}(\text{I})$ to form a new $\text{Cu}(\text{I})$ complex. The energy transfer from the excited $\text{Ir}(\text{ppy})_3$ to the Cu intermediate dominates the reaction pathway. The reaction between the triplet $\text{Cu}(\text{I})$ complex and phenyl iodides formed the Ullmann coupling product and

closed the $\text{Cu}(\text{I})$ -based redox cycle. Recently, Hanson disclosed that protonation of a silylenol ether with *N*-hydroxysuccinimide could be triggered by visible light in the presence of 7-bromo-2-naphthol and FIrpic [78]. Using *N*-hydroxysuccinimide as the sacrificial proton source, the protonated 7-bromo-2-naphthol transforms to the corresponding triplet state by the energy transfer from the excited FIrpic. Subsequent proton transfer from the highly acidic triplet state of 7-bromo-2-naphthol to silylenol ether provided ketone and regenerated 7-bromo-2-naphthol.

VISIBLE-LIGHT-DRIVEN ASYMMETRIC SYNTHESIS

A large variety of methods have been developed for asymmetric thermal reactions. On the other hand, asymmetric photoreactions have not enjoyed the same level of success as thermal reactions. Upon excitation by light, the high-energy intermediates often undergo a fast subsequent reaction that can be difficult to influence with an exogenous asymmetric catalyst. With the recent great successes in visible-light-driven reactions and an increasing understanding the reaction mechanism, visible-light-driven asymmetric synthesis has recently undergone a significant renaissance.

In 2008, MacMillan developed a dual photoredox organocatalytic protocol for the enantioselective α -alkylation of aldehydes with α -bromo carbonyls (Fig. 5a) [79]. In this transformation, in-situ condensation of imidazolidinone catalyst AC1 with an aldehyde delivered nucleophilic chiral enamine. Single-electron reduction of α -bromo carbonyls by the $\text{Ru}(\text{I})$ complex-based photoredox cycle generated electrophilic radical species, which could attack the *Si*-face of the enamine with highly stereoselectivity. The α -amino radical underwent single-electron oxidation and hydrolysis, thereby affording enantio-enriched α -alkyl aldehyde product. This strategy has subsequently been exploited by many research groups and has resulted in the development of a diverse range of asymmetric α -functionalization reactions such as trifluoromethylation [80], benzylation [81] and cyanoalkylation [82]. In 2014, Meggers and co-workers reported that chiral-at-metal iridium complexes play a dual role as both a Lewis acid and a photocatalyst in the enantioselective α -alkylation of 2-acylimidazoles with electron-deficient benzyl halides (Fig. 5a) [83]. The iridium catalyst first binds to an acyl imidazole compound, creating a structurally well-defined enolate complex. The $\text{Ir}(\text{III})$ enolate complex is photoactive for visible

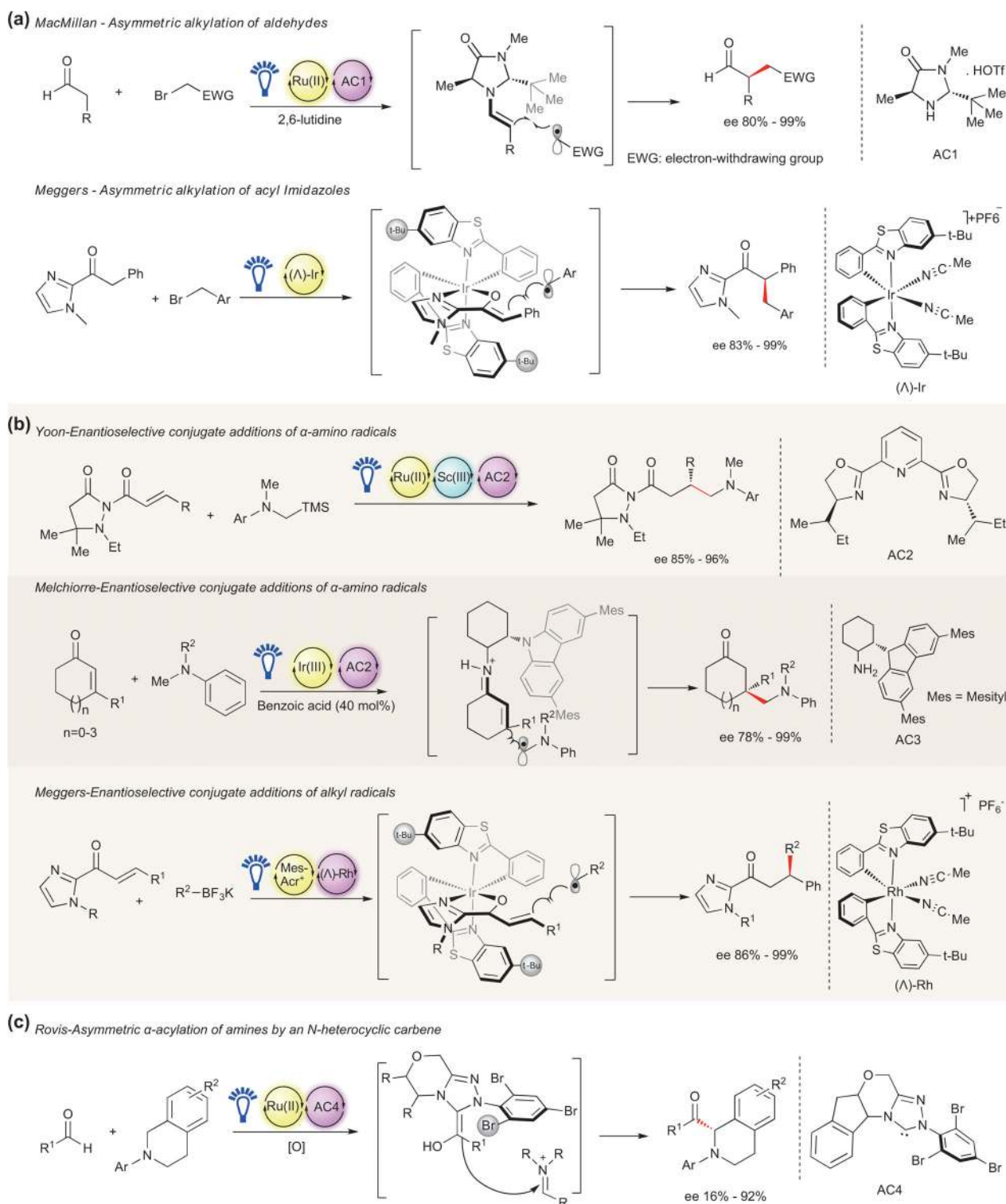


Figure 5. Visible-light-driven asymmetric synthesis. (a) Asymmetric α -functionalization of aldehydes and ketones; (b) asymmetric conjugate additions; (c) asymmetric α -functionalization of amines; (d) asymmetric radical coupling and ketyl radical-mediated enantioselective reactions; (e) asymmetric photocatalytic [2 + 2] cycloadditions.

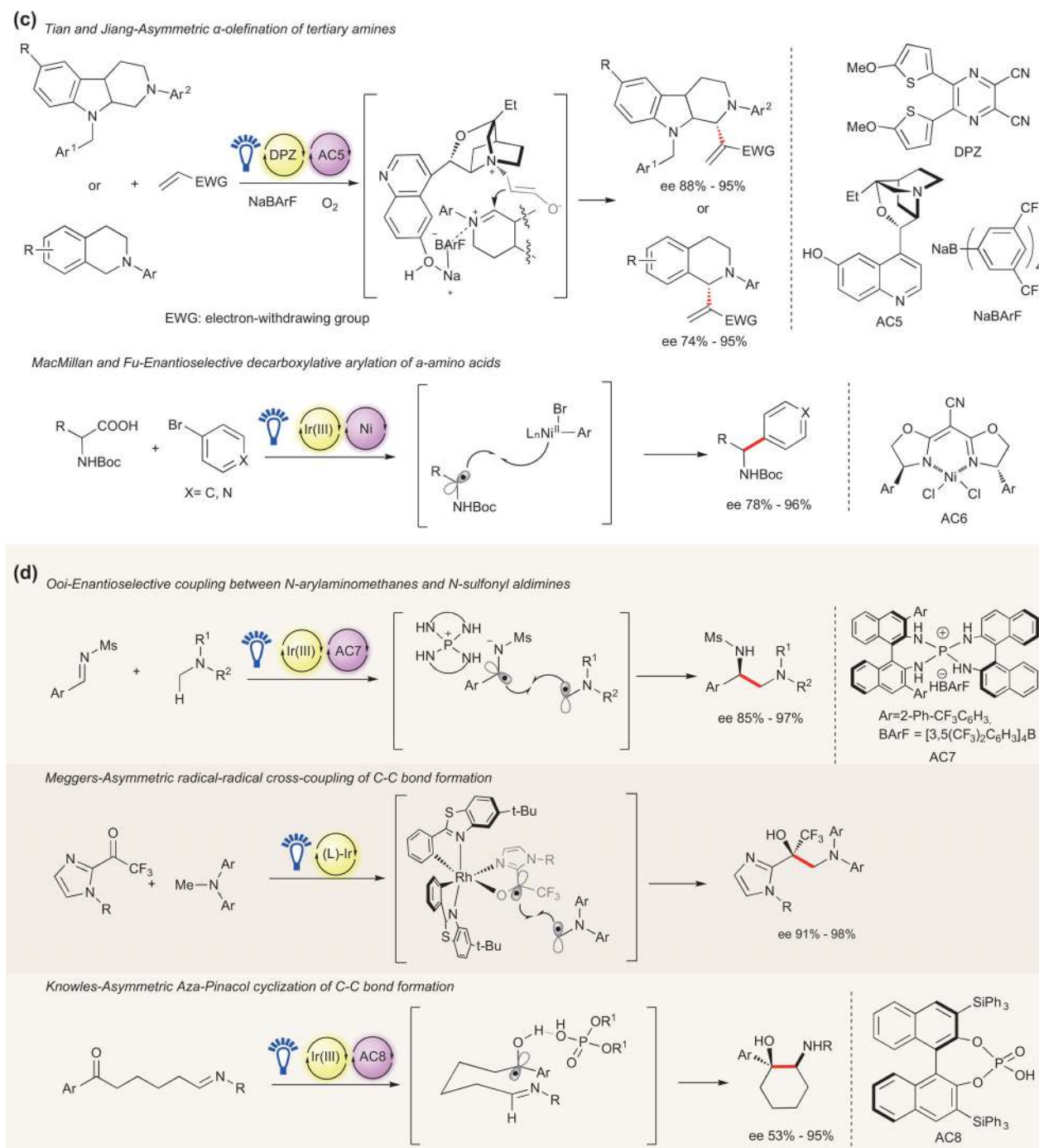


Figure 5. Continued.

light and photoexcitation of this complex promotes one-electron reduction of a benzylic halide to afford an electrophilic radical intermediate. This radical intercepts another equivalent of the enolate complex, resulting in the formation of a new carbon-carbon bond with exceptionally high levels of stereocontrol. Since this initial publication, they have been able to expand this mechanistic platform

to a wide range of asymmetric α -functionalization reactions, including trichloromethylations [84], aminoalkylation [85,86] and amination [87].

Recently, Yoon and co-workers disclosed that conjugate additions of α -aminoalkyl radicals could be rendered asymmetric through the use of a chiral bioxazolyl pyridine-ligated Lewis acid catalyst (Fig. 5b) [88]. Here, photoredox catalysis mediates

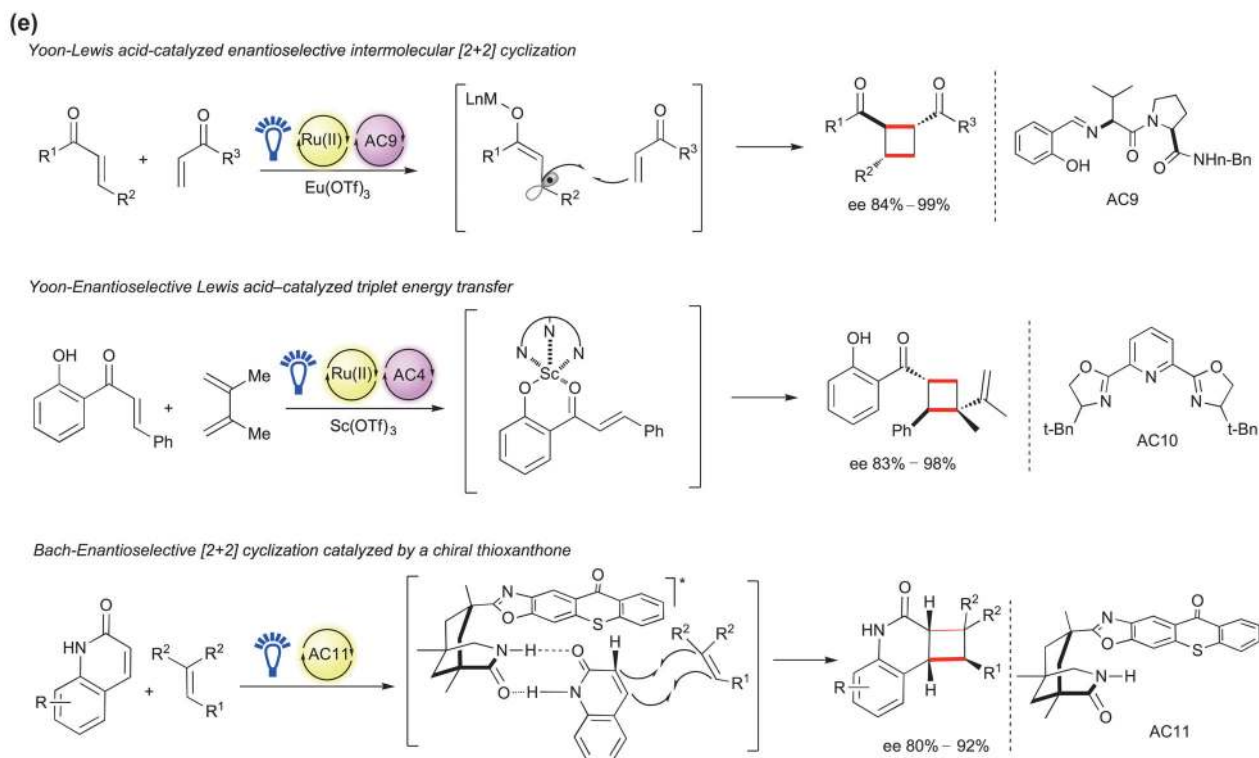


Figure 5. Continued.

the generation of the α -aminoalkyl radical and the Lewis acid complex controls stereoselectivity in the subsequent addition step. The merger of photoredox catalysis with other organocatalytic activation modes has expanded the repertoire of carbon–carbon and carbon–heteroatom bond-forming reactions that can be accomplished using this dual catalytic strategy. Of particular note is a report by Melchiorre and co-workers demonstrating that the long-established LUMO-lowering strategy of iminium catalysis was able to expand to asymmetric conjugate additions of α -aminoalkyl radicals (Fig. 5b) [89]. In this seminal work, chiral primary amine catalyst AC3 was employed to deliver the corresponding iminium and preclude an undesirable β -scission event. Stereoselective attack of the chiral iminium by the α -aminoalkyl radicals constructed a challenging quaternary carbon stereocenter, providing the repertoire of asymmetric conjugate additions of α,β -unsaturated ketones with easily available *N*-arylamines. In a concomitant report, Meggers and co-workers found a dual photoredox Lewis acid-catalysed conjugate addition reaction that utilizes organotrifluoroborate salts as the source of the alkyl radical coupling partner (Fig. 5b) [90]. In this protocol, an organic dye Mes-Acr⁺ was employed to mediate formation of the requisite alkyl radical and high levels of enantioselectivity

was achieved using a chiral-at-metal rhodium complex as the asymmetric catalyst.

Asymmetric α -functionalization of amines by visible light has also been impressively established. Rovis and co-workers demonstrated that the catalytic asymmetric α -acylation of tertiary amines with aldehydes facilitated by the combination of chiral *N*-heterocyclic carbene catalysis and photoredox catalysis (Fig. 5c) [91]. In-situ generation of a Breslow-type intermediate was accomplished using a chiral *N*-heterocyclic carbene catalyst (AC4). The visible-light-driven dehydrogenation of tertiary amines using *m*-dinitrobenzene as the oxidant generated corresponding iminium ion. Subsequent trapping of the electrophilic iminium ion with this catalytic intermediate resulted in the formation of the α -amino ketone products with high levels of enantioselectivity. Recently, asymmetric α -olefination of tertiary amines employing a triple-catalyst strategy was disclosed by Tian and Jiang. By combining an organophotocatalyst, a dicyanopyrazine-derived chromophore DPZ, a chiral Lewis base catalyst, AC5 and an inorganic salt cocatalyst, NaBARF, the photoreaction proceeded efficiently in the presence of molecular oxygen, providing straightforward access to a series of valuable α -substituted tetrahydro- β -carbolines and tetrahydroisoquinolines with excellent enantioselectivities (Fig. 5c) [92]. Prior

to this report, Stephenson and Jacobsen showed that enantioselective α -alkylation of tetrahydroisoquinolines could be accomplished with silyl ketene acetals using a dual photoredox chiral thiourea catalyst system through binding of the thiourea catalyst to the tightly associated halide counterion of the iminium ion [93]. More recently, MacMillan and Fu demonstrated that dual photoredox chiral Ni catalysis could enable decarboxylative arylation of α -amino acids with useful levels of enantioselectivity [94]. Here, NiCl_2 and a bis(oxazoline) ligand were employed to generate chiral Ni catalysis AC6 in situ, which could react with an aryl halide giving Ni(II) –aryl complex. The α -aminoalkyl radical, formed by photocatalyst-mediated oxidation and decarboxylation of an α -amino acid, could be trapping by the chiral Ni(II) –aryl complex. The resulting diorganonickel(III) adduct would then undergo reductive elimination to afford the desired benzylic amines in a highly enantioselective manner.

Seminal studies from Ooi and co-workers described a unique mechanistic pathway for the highly enantioselective synthesis of diamines from *N*-sulfonylaldimines and *N*-arylaminoethanes (Fig. 5d) [95]. The key radical–radical coupling step was rendered asymmetric via the formation of a chiral ion pair consisting of the prochiral radical anion, resulting from single-electron reduction of a *N*-sulfonylaldimine, and a chiral aminophosphonium ion AC7. Here, chiral ion AC7 governs the enantiofacial approach of the oxidatively generated *N*-aryl α -amino radical. In a further demonstration of the utility of the stereoselective iridium catalyst described in Fig. 5a, the Meggers laboratory found that the visible-light-driven synthesis of chiral 1,2-amino alcohols by a radical–radical cross-coupling reaction could be catalysed by the chiral-at-metal iridium complex (Fig. 5d) [96]. The proposed mechanism indicated that the resulting stabilized ketyl radical is a persistent radical that possesses relatively little propensity towards homodimerization. The photogenerated amine radical interacts with the persistent ketyl radical within the chiral environment of the Ir complex, which provides impressively high enantioselectivity. In another report of ketyl radical-mediated asymmetric synthesis, Knowles and co-workers demonstrated that the reductive proton-coupled electron-transfer strategy could be used to effect an asymmetric intramolecular aza-pinacol reaction through the use of chiral phosphoric acid catalyst AC8 (Fig. 5d) [97]. Herein, aryl ketones could be reduced to the corresponding ketyl radical through the cooperative action of a photoredox catalyst and a phosphate H-bond donor. The high enantioselectivities

arise from the tight bonding between the chiral catalyst AC8 and the ketyl radical during the intramolecular radical cyclization.

The first example of visible-light-driven enantioselective $[2 + 2]$ cyclization was reported in 2014 by the Yoon group. Utilizing Eu(OTf)_3 with dipeptide-derived chiral ligand AC9 led to formation of the 1,2-*trans*-isomers of the cyclobutanes with high levels of enantiocontrol (Fig. 5e) [98]. In this protocol, successful electron transfer to an enone required the coordination of the enone to the chiral Lewis acid. The generated radical anion in the presence of the chiral Lewis acid added enantioselectively to another enone. Importantly, the relative configuration of the products could be controlled by the chiral ligand of the Lewis acid. The requirement of the Lewis acid for both reactivity and stereoselectivity prevented detrimental racemic background cycloadditions from occurring. In a subsequent report, Yoon demonstrated that asymmetric $[3 + 2]$ cycloadditions involving cyclopropyl ketones could be achieved using a similar strategy [99]. As discussed in the section of visible-light-driven synthesis by energy-transfer processes, the triplet-state alkenes produced by the triplet–triplet energy transfer are excited molecules with a short lifetime. Therefore, the stereocontrols of the $[2 + 2]$ cyclization with the triplet-state alkenes are particularly difficult. More recently, Blum and co-workers found that Lewis acid coordination dramatically lowers the triplet energy of 2'-hydroxychalcones. Thus, the energy transfer from the excited photocatalyst to a chiral Lewis acid coordinated chalcone produced a triplet chiral compound, which could undergo cross cycloaddition in a highly enantioselective manner (Fig. 5e) [100]. This activation mode provides a strategy for stereocontrols of asymmetric reactions involving electronically excited states.

Bath and co-workers found a chiral thioxanthone AC11 (Fig. 5e) is able to catalyse asymmetric $[2 + 2]$ photocycloaddition of quinolone using visible light. The association between the chiral thioxanthone and the quinolones by hydrogen bonding is critical for the success of the reaction. Under visible irradiation, the energy transfer from the triplet thioxanthone to the quinolone gave the triplet quinolone in a chiral environment, thereby delivering enantioselective cycloadduct. In 2014, the chiral thioxanthone AC11 was synthesized and applied to the reaction of substituted 4-(pent-4-enyl)quinolones and their heteroanalogues [101]. The reaction proceeded with outstanding enantioselectivities under visible-light irradiation and delivered the photoproducts. Later on, enantioselective intermolecular $[2 + 2]$ photocycloaddition of quinolones with a variety of olefins under

visible-light irradiation was achieved by employing AC11 as the chiral photocatalyst (Fig. 5e) [102]. Despite this similarity, the design principle is conceptually novel as the metal complex is also responsible for the face differentiation so that the addition of the formed alkyl radicals to the enolate occurs with high enantioselectivity.

CONCLUSIONS

Over the past decade, observations made in visible-light-driven organic reactions strongly demonstrate that modern photochemistry has a substantial impact on the field of chemical synthesis by providing a complementary strategy for the activation of organic substrates. Both electron-transfer and energy-transfer photocatalysis have been used to generate classes of reactive intermediates whose general reactivity patterns are well understood, inspiring the design of a wide range of new chemical reactions. The increasing demands for environmentally benign and energy-saving industrial processes have motivated photochemists to seek new strategies from the adjacent research fields such as organotransition metal chemistry, biocatalysis and energy chemistry. The recent development of dual photoredox catalytic platforms has proven uniquely effective for the design of novel synthetic transformations and provided new activation modes that enable synthetic transformations to proceed in a highly regio- and enantioselective manner.

Despite these advances, we feel that many exciting opportunities and challenges still lay ahead the field of visible-light-driven transformations. For instance, the stereocontrol of visible-light-driven reactions is difficult to be realized; in most cases, the reactions are performed with very low quantum yields; the mechanisms of some dual catalytic reactions are still unclear; and the chemoselectivities in short-lived intermediate-mediated photoreactions are unsatisfactory for industrial processes. In this regard, Ciamician's grand vision has yet to be fully realized and the development of many more impressive visible-light-mediated strategies is highly desirable for the future.

FUNDING

We are grateful for financial support from the Ministry of Science and Technology of China (2013CB834804, 2013CB834505 and 2014CB239402), the National Natural Science Foundation of China (21572090, 21390404 and 91427303), the Strategic Priority Research Program of the Chinese Academy of Sciences (XDB17030200) and the Chinese Academy of Sciences.

Conflict of interest statement. None declared.

REFERENCES

1. Ciamician G. The photochemistry of the future. *Science* 1912; **36**: 385–94.
2. Special issue: photoredox catalysis in organic chemistry. *Acc Chem Res* 2016; **49**.
3. Special issue: photochemistry in organic synthesis. *Chem Rev* 2016; **116**: 9629–10342.
4. Condie AG, González-Gómez JC and Stephenson CRJ. Visible-light photoredox catalysis: aza-Henry reactions via C–H functionalization. *J Am Chem Soc* 2010; **132**: 1464–5.
5. Rueping M, Vila C and Koenigs RM *et al.* Dual catalysis: combining photoredox and Lewis base catalysis for direct Mannich reactions. *Chem Commun* 2011; **47**: 2360–2.
6. Zou YQ, Lu LQ and Xiao WJ *et al.* Visible-light-induced oxidation/[3 + 2] cycloaddition/oxidative aromatization sequence: a photocatalytic strategy to construct pyrrolo[2,1-*a*] isoquinolines. *Angew Chem Int Ed* 2011; **50**: 7171–5.
7. Hari DP and König B. Eosin Y catalyzed visible light oxidative C–C and C–P bond formation. *Org Lett* 2011; **13**: 3852–5.
8. Pan YH, Kee CW and Tan CH *et al.* Dehydrogenative coupling reactions catalysed by Rose Bengal using visible light irradiation. *Green Chem* 2011; **13**: 2682–5.
9. Liu Q, Li Y-N and Wu LZ *et al.* Reactivity and mechanistic insight into visible-light-induced aerobic cross-dehydrogenative coupling reaction by organophotocatalysts. *Chem Eur J* 2012; **18**: 620–7.
10. Zhong J-J, Meng QY and Wu LZ *et al.* A highly efficient and selective aerobic cross-dehydrogenative-coupling reaction photocatalyzed by a platinum(II) terpyridyl complex. *Chem Eur J* 2013; **19**: 6443–50.
11. Bartling H, König B and Gschwind RM. The photocatalyzed aza-Henry reaction of *N*-aryltetrahydroisoquinolines: comprehensive mechanism, H- versus H⁺-abstraction, and background reactions. *J Am Chem Soc* 2016; **138**: 11860–71.
12. Rueping M and Vila C. Visible light photoredox-catalyzed multicomponent reactions. *Org Lett* 2013; **15**: 2092–5.
13. Gao X-W, Meng QY and Wu LZ *et al.* Combining visible light catalysis and transition metal catalysis for the alkylation of secondary amines. *Adv Synth Catal* 2013; **355**: 2158–64.
14. Hou H, Zhu SQ and Rueping M *et al.* Visible-light photoredox-catalyzed synthesis of nitrones: unexpected rate acceleration by water in the synthesis of isoxazolidines. *Org Lett* 2014; **16**: 2872–5.
15. Dinnocenzo JP and Banach TE. Deprotonation of tertiary amine cation radicals: a direct experimental approach. *J Am Chem Soc* 1989; **111**: 8646–53.
16. Zhang XM, Yeh SR and Mariano PS *et al.* Dynamics of α -CH deprotonation and α -desilylation reactions of tertiary amine cation radicals. *J Am Chem Soc* 1994; **116**: 4211–20.

17. Ju XH, Yu W and Bian FL *et al.* The reaction of tertiary anilines with maleimides under visible light redox catalysis. *Adv Synth Catal* 2012; **354**: 356–7.
18. Zhu SQ, Das A and Rueping M *et al.* Oxygen switch in visible-light photoredox catalysis: radical additions and cyclizations and unexpected C–C bond cleavage reactions. *J Am Chem Soc* 2013; **135**: 1823–9.
19. Zhang P, Xiao TB and Zhou L *et al.* Synthesis of 3-acylindoles by visible-light induced intramolecular oxidative cyclization of *o*-alkynylated *N,N*-dialkylamines. *Org Lett* 2014; **16**: 3264–7.
20. Maity S and Zheng N. A visible-light-mediated oxidative C–N bond formation/aromatization cascade: photocatalytic preparation of *N*-arylindoles. *Angew Chem Int Ed* 2012; **51**: 9562–6.
21. Musacchio AJ, Nguyen LQ and Knowles RR *et al.* Catalytic olefin hydroamination with aminium radical cations: a photoredox method for direct C–N bond formation. *J Am Chem Soc* 2014; **136**: 12217–20.
22. Cai SY, Li ZG and Wang DZG *et al.* Visible-light-promoted C–C bond cleavage: photocatalytic generation of iminium ions and amino radicals. *Angew Chem Int Ed* 2012; **51**: 8050–3.
23. Xie J, Xue QC and Zhu CJ *et al.* A visible-light-promoted aerobic C–H/C–N cleavage cascade to isoxazolidine skeletons. *Chem Sci* 2013; **4**: 1281–6.
24. Zou YQ, Jørgensen KA and Xiao WJ *et al.* Highly efficient aerobic oxidative hydroxylation of arylboronic acids: photoredox catalysis using visible light. *Angew Chem Int Ed* 2012; **51**: 784–8.
25. Pitre SP, McTiernan CD and Scaian JC *et al.* Mechanistic insights and kinetic analysis for the oxidative hydroxylation of arylboronic acids by visible light photoredox catalysis: a metal-free alternative. *J Am Chem Soc* 2013; **135**: 13286–9.
26. An J, Zou YQ and Xiao WJ *et al.* Visible light-induced aerobic oxyamidation of indoles: a photocatalytic strategy for the preparation of tetrahydro-5*H*-indolo [2,3-*b*]quinolins. *Adv Synth Catal* 2013; **355**: 1483–9.
27. Zhang ML, Duan YQ and Zhu CJ *et al.* Visible-light-induced aerobic dearomative reaction of indole derivatives: access to heterocycle fused or spirocyclic indolones. *Chem Commun* 2016; **52**: 4761–3.
28. Sun HN, Yang C and Xia WJ *et al.* Oxidative C–C bond cleavage of aldehydes via visible-light photoredox catalysis. *Org Lett* 2013; **15**: 624–7.
29. Clennana EL and Pace A. Advances in singlet oxygen chemistry. *Tetrahedron* 2005; **61**: 6665–91.
30. Alberti MN, Vougioukalakis GC and Orfanopoulos M. Photosensitized oxidations of substituted pyrroles: unanticipated radical-derived oxygenated products. *J Org Chem* 2009; **74**: 7274–82.
31. Li J, Cai SY and Wang DZG *et al.* Visible light induced photocatalytic conversion of enamines into amides. *Synlett* 2014; **25**: 1626–8.
32. Fan WG and Li PX. Visible-light-mediated 1,2-acyl migration: the reaction of secondary enamino ketones with singlet oxygen. *Angew Chem Int Ed* 2014; **53**: 12201–4.
33. Meng QY, Lei T and Wu LZ *et al.* A unique 1,2-acyl migration for the construction of quaternary carbon by visible light irradiation of platinum(II) polypyridyl complex and molecular oxygen. *Org Lett* 2014; **16**: 5968–71.
34. Cao S, Zhong SS and Wan JP *et al.* Visible-light-induced C=C bond cleavage of enamines for the synthesis of 1,2-diketones and quinoxalines in sustainable medium. *ChemCatChem* 2015; **7**: 1478–82.
35. Zhang Q-B, Wu LZ and Liu Q *et al.* Preparation of α -acyloxy ketones via visible-light-driven aerobic oxo-acyloxylation of olefins with carboxylic acids. *Org Lett* 2016; **18**: 5256–9.
36. Su YJ, Zhang LR and Jiao N. Utilization of natural sunlight and air in the aerobic oxidation of benzyl halides. *Org Lett* 2011; **13**: 2168–71.
37. Yi H, Bian CL and Lei AW *et al.* Visible light mediated efficient oxidative benzylic sp³ C–H to ketone derivatives obtained under mild conditions using O₂. *Chem Commun* 2015; **51**: 14046–9.
38. Lin SS, Ischay MA and Yoon TP *et al.* Radical cation Diels–Alder cycloadditions by visible light photocatalysis. *J Am Chem Soc* 2011; **133**: 19350–3.
39. Ischay MA, Ament MS and Yoon TP. Crossed intermolecular [2 + 2] cycloaddition of styrenes by visible light photocatalysis. *Chem Sci* 2012; **3**: 2807–11.
40. Parrish JD, Ischay MA and Yoon TP *et al.* Endoperoxide synthesis by photocatalytic aerobic [2 + 2 + 2] cycloadditions. *Org Lett* 2012; **14**: 1640–3.
41. Lu Z, Parrish JD and Yoon TP. [3 + 2] Photooxygenation of aryl cyclopropanes via visible light photocatalysis. *Tetrahedron* 2014; **70**: 4270–8.
42. Song T, Liu Q and Wang Y *et al.* Aerobic oxidative coupling of resveratrol and its analogues by visible light using mesoporous graphitic carbon nitride (mpg-C₃N₄) as a bioinspired catalyst. *Chem Eur J* 2014; **20**: 678–82.
43. Wang L, Wu LZ and Liu Q *et al.* Synthesis of 2-substituted pyrimidines and benzoxazoles via a visible-light-driven organocatalytic aerobic oxidation: enhancement of the reaction rate and selectivity by a base. *Green Chem* 2014; **16**: 3752–7.
44. Wei XJ, Wu LZ and Liu Q *et al.* Metal-free-mediated oxidation aromatization of 1,4-dihydropyridines to pyridines using visible light and air. *Chin J Chem* 2014; **32**: 1245–50.
45. Dempsey JL, Brunschwig BS and Winkler JR *et al.* Hydrogen evolution catalyzed by cobaloximes. *Acc Chem Res* 2009; **42**: 1995–2004.
46. Zhang D, Wu LZ and Zhou L *et al.* Photocatalytic hydrogen production from hantzsch 1,4-dihydropyridines by platinum(II) terpyridyl complexes in homogeneous solution. *J Am Chem Soc* 2004; **126**: 3440–1.
47. Wang DH, Peng ML and Han Y *et al.* Facile preparation of 3,4-diarylpyrroles and hydrogen by a platinum(III) terpyridyl complex. *Inorg Chem* 2009; **48**: 9995–7.
48. Chen ZY, Wang DH and Chen B *et al.* Visible light-induced synthesis of 3,4-diarylthiophenes from 3,4-diaryl-2,5-dihydrothiophenes. *J Org Chem* 2012; **77**: 6773–7.
49. Ye P, Wang DH and Chen B *et al.* Visible light catalyzed aromatization of 1,3,5-triaryl-2-pyrazolines by platinum(II) polypyridyl complex under oxidant-free condition. *Sci China Chem* 2016; **59**: 175–9.
50. Meng QY, Zhong JJ and Liu Q *et al.* A cascade cross-coupling hydrogen evolution reaction by visible light catalysis. *J Am Chem Soc* 2013; **135**: 19052–5.
51. Zhong JJ, Meng QY and Liu B *et al.* Cross-coupling hydrogen evolution reaction in homogeneous solution without noble metals. *Org Lett* 2014; **16**: 1988–91.
52. Gao XW, Meng QY and Li JX *et al.* Visible light catalysis assisted site-specific functionalization of amino acid derivatives by C–H bond activation without oxidant: cross-coupling hydrogen evolution reaction. *Acc Catal* 2015; **5**: 2391–6.
53. Xiang M, Meng QY and Li JX *et al.* Activation of C–H bonds through oxidant-free photoredox catalysis: cross-coupling hydrogen-evolution transformation of isochromans and β -keto esters. *Chem Eur J* 2015; **21**: 18080–4.
54. Zhang GT, Liu C and Yi H *et al.* External oxidant-free oxidative cross-coupling: a photoredox cobalt-catalyzed aromatic C–H thiolation for constructing C–S bonds. *J Am Chem Soc* 2015; **137**: 9273–80.
55. Wu CJ, Meng QY and Lei T *et al.* An oxidant-free strategy for indole synthesis via intramolecular C–C bond construction under visible light irradiation: cross-coupling hydrogen evolution reaction. *Acc Catal* 2016; **6**: 4635–9.
56. Zheng YW, Chen B and Ye P *et al.* Photocatalytic hydrogen-evolution cross-couplings: benzene C–H amination and hydroxylation. *J Am Chem Soc* 2016; **138**: 10080–3.

57. Zhang GT, Hu X and Chiang CW *et al.* Anti-Markovnikov oxidation of β -alkyl styrenes with H_2O as the terminal oxidant. *J Am Chem Soc* 2016; **138**: 12037–40.
58. Yi H, Niu LB and Song CL *et al.* Photocatalytic dehydrogenative cross-coupling of alkenes with alcohols or azoles without external oxidant. *Angew Chem Int Ed* 2015; **54**: 1120–4.
59. Zhang GT, Zhang LL and Yi H *et al.* Visible-light induced oxidant-free oxidative cross-coupling for constructing allylic sulfones from olefins and sulfinic acids. *Chem Commun* 2016; **52**: 10407–10.
60. Li XB, Li ZJ and Gao YJ *et al.* Mechanistic insights into the interface-directed transformation of thiols into disulfides and molecular hydrogen by visible-light irradiation of quantum dots. *Angew Chem Int Ed* 2014; **53**: 2085–9.
61. Chai ZG, Zeng TT and Li Q *et al.* Efficient visible light-driven splitting of alcohols into hydrogen and corresponding carbonyl compounds over a Ni-modified CdS photocatalyst. *J Am Chem Soc* 2016; **138**: 10128–31.
62. Luo K, Chen YZ and Yang WC *et al.* Cross-coupling hydrogen evolution by visible light photocatalysis toward $C(sp^2)$ -P formation: metal-free C-H functionalization of thiazole derivatives with diarylphosphine oxides. *Org Lett* 2016; **18**: 452–5.
63. Turro NJ. Energy transfer processes. *Pure Appl Chem* 1977; **49**: 405–29.
64. Wrighton M and Markham J. Quenching of the luminescent state of tris(2,2'-bipyridine)ruthenium(II) by electronic energy transfer. *J Phys Chem* 1973; **77**: 3042–4.
65. Ikezawa H, Kutal C and Yasufuku K *et al.* Direct and sensitized valence photoisomerization of a substituted norbornadiene. Examination of the disparity between singlet- and triplet-state reactivities. *J Am Chem Soc* 1986; **108**: 1589–94.
66. Lin QY, Xu XH and Qing FL. Chemo-, regio-, and stereoselective trifluoromethylation of styrenes via visible light-driven single-electron transfer (SET) and triplet-triplet energy transfer (TTET) processes. *J Org Chem* 2014; **79**: 10434–46.
67. Osawa M, Hoshino M and Wakatsuki Y. A light-harvesting *tert*-phosphane ligand bearing a ruthenium(II) polypyridyl complex as substituent. *Angew Chem Int Ed* 2001; **40**: 3472–4.
68. Islangulov RR and Castellano FN. Photochemical upconversion: anthracene dimerization sensitized to visible light by a Rull chromophore. *Angew Chem Int Ed* 2006; **45**: 5957–9.
69. Nitadori H, Takahashi T and Inagaki A *et al.* Enhanced photocatalytic activity of α -methylstyrene oligomerization through effective metal-to-ligand charge-transfer localization on the bridging ligand. *Inorg Chem* 2012; **51**: 51–62.
70. Zou YQ, Duan SW and Meng XG *et al.* Visible light induced intermolecular [2 + 2]-cycloaddition reactions of 3-ylideneoxindoles through energy transfer pathway. *Tetrahedron* 2012; **68**: 6914–9.
71. Lu Z and Yoon TP. Visible light photocatalysis of [2 + 2] styrene cycloadditions by energy transfer. *Angew Chem Int Ed* 2012; **51**: 10329–32.
72. Hurlley AE, Lu Z and Yoon TP. [2 + 2] Cycloaddition of 1,3-dienes by visible light photocatalysis. *Angew Chem Int Ed* 2014; **53**: 8991–4.
73. Liu Q, Zhu FP and Jin XL *et al.* Visible-light-driven intermolecular [2 + 2] cycloadditions between coumarin-3-carboxylates and acrylamide analogs. *Chem Eur J* 2015; **21**: 10326–9.
74. Farney EP and Yoon TP. Visible-light sensitization of vinyl azides by transition-metal photocatalysis. *Angew Chem Int Ed* 2014; **53**: 793–7.
75. Scholz SO, Farney EP and Kim S *et al.* Spin-selective generation of triplet nitrenes: olefin aziridination through visible-light photosensitization of azidoformates. *Angew Chem Int Ed* 2016; **55**: 2239–42.
76. Brachet E, Ghosh T and Ghosh I *et al.* Visible light C–H amidation of heteroarenes with benzoyl azides. *Chem Sci* 2015; **6**: 987–92.
77. Yoo WJ, Tsukamoto T and Kobayashi S. Visible light-mediated Ullmann-type C–N coupling reactions of carbazole derivatives and aryl iodides. *Org Lett* 2015; **17**: 3640–2.
78. Das A, Banerjee T and Hanson K. Protonation of silylenol ether via excited state proton transfer catalysis. *Chem Commun* 2016; **52**: 1350–3.
79. Nicewicz DA and MacMillan DWC. Merging photoredox catalysis with organocatalysis: the direct asymmetric alkylation of aldehydes. *Science* 2008; **322**: 77–80.
80. Nagib DA, Scott ME and MacMillan DWC. Enantioselective α -trifluoromethylation of aldehydes via photoredox organocatalysis. *J Am Chem Soc* 2009; **131**: 10875–7.
81. Shih HW, Vander Wal MN and MacMillan DWC *et al.* Enantioselective α -benzylation of aldehydes via photoredox organocatalysis. *J Am Chem Soc* 2010; **132**: 13600–3.
82. Welin ER, Warkentin AA and MacMillan DWC *et al.* Enantioselective α -alkylation of aldehydes by photoredox organocatalysis: rapid access to pharmacophore fragments from β -cyanoaldehydes. *Angew Chem Int Ed* 2015; **54**: 9668–72.
83. Huo H, Shen X and Meggers E *et al.* Asymmetric photoredox transition-metal catalysis activated by visible light. *Nature* 2014; **515**: 100–3.
84. Huo H, Wang C and Meggers E *et al.* Enantioselective, catalytic trichloromethylation through visible-light-activated photoredox catalysis with a chiral iridium complex. *J Am Chem Soc* 2015; **137**: 9551–4.
85. Wang C, Zheng Y and Meggers E *et al.* Merger of visible light induced oxidation and enantioselective alkylation with a chiral iridium catalyst. *Chem Eur J* 2015; **21**: 7355–9.
86. Tan Y, Yuan W and Meggers E *et al.* Aerobic asymmetric dehydrogenative cross-coupling between two C_{sp^3} -H groups catalyzed by a chiral-at-metal rhodium complex. *Angew Chem Int Ed* 2015; **54**: 13045–8.
87. Huang X, Webster RD and Meggers E *et al.* Asymmetric catalysis with organic azides and diazo compounds initiated by photoinduced electron transfer. *J Am Chem Soc* 2016; **138**: 12636–42.
88. Ruiz Espelt L, McPherson IS and Yoon TP *et al.* Enantioselective conjugate additions of α -amino radicals via cooperative photoredox and Lewis acid catalysis. *J Am Chem Soc* 2015; **137**: 2452–5.
89. Murphy JJ, Bastida D and Melchiorre P *et al.* Asymmetric catalytic formation of quaternary carbons by iminium ion trapping of radicals. *Nature* 2016; **532**: 218–22.
90. Huo H, Harms K and Meggers E *et al.* Catalytic, enantioselective addition of alkyl radicals to alkenes via visible-light-activated photoredox catalysis with a chiral rhodium complex. *J Am Chem Soc* 2016; **138**: 6936–9.
91. DiRocco DA and Rovis T. Catalytic asymmetric α -acylation of tertiary amines mediated by a dual catalysis mode: N-heterocyclic carbene and photoredox catalysis. *J Am Chem Soc* 2012; **134**: 8094–7.
92. Wei G, Zhang C and Jiang ZY *et al.* Enantioselective aerobic oxidative $C(sp^3)$ -H olefination of amines via cooperative photoredox and asymmetric catalysis. *ACS Catal* 2016; **6**: 3708–12.
93. Bergonzini G, Schindler CS and Stephenson CRJ *et al.* Photoredox activation and anion binding catalysis in the dual catalytic enantioselective synthesis of β -amino esters. *Chem Sci* 2014; **5**: 112–6.
94. Zuo Z, Fu GC and MacMillan DWC *et al.* Enantioselective decarboxylative arylation of α -amino acids via the merger of photoredox and nickel catalysis. *J Am Chem Soc* 2016; **138**: 1832–5.

95. Uraguchi D, Kinoshita N and Ooi T *et al.* Synergistic catalysis of ionic Brønsted acid and photosensitizer for a redox neutral asymmetric α -coupling of *N*-arylaminoethanes with aldimines. *J Am Chem Soc* 2015; **137**: 13768–71.
96. Wang C, Qin J and Meggers E *et al.* Asymmetric radical–radical cross-coupling through visible-light-activated iridium catalysis. *Angew Chem Int Ed* 2016; **55**: 685–8.
97. Rono LJ, Yayla HG and Knowles RR *et al.* Enantioselective photoredox catalysis enabled by proton-coupled electron transfer: development of an asymmetric aza-pinacol cyclization. *J Am Chem Soc* 2013; **135**: 17735–8.
98. Du J, Skubi KL and Yoon TP *et al.* A dual-catalysis approach to enantioselective [2 + 2] photocycloadditions using visible light. *Science* 2014; **344**: 392–6.
99. Amador AG, Sherbrook EM and Yoon TP. Enantioselective photocatalytic [3 + 2] cycloadditions of aryl cyclopropyl ketones. *J Am Chem Soc* 2016; **138**: 4722–5.
100. Blum TR, Miller ZD and Yoon TP *et al.* Enantioselective photochemistry through Lewis acid-catalyzed triplet energy transfer. *Science* 2016; **354**: 1391–5.
101. Tröster A, Alonso R and Bach T *et al.* Enantioselective intermolecular [2 + 2] photocycloaddition reactions of 2(1H)-quinolones induced by visible light irradiation. *J Am Chem Soc* 2016; **138**: 7808–11.
102. Alonso R and Bach T. A chiral thioxanthone as an organocatalyst for enantioselective [2 + 2] photocycloaddition reactions induced by visible light. *Angew Chem Int Ed* 2014; **53**: 4368–71.